Guidelines on Foundation Loading and Deformation Due to Liquefaction Induced Lateral Spreading

January, 2012

1 INTRODUCTION

Past earthquakes offer many examples of bridges that either collapsed or incurred severe damage resulting from lateral foundation movement caused by liquefaction induced lateral spreading. The following guidelines provide specific recommendations for the calculation of loads and deformation demands on bridge foundations and abutments resulting from liquefaction induced spreading ground. These procedures are based on recommendations given in Ashford et al. (2010) but occasionally go beyond these more general recommendations in an effort to provide as specific guidance as possible. The recommended approach relies on an equivalent nonlinear static analysis methodology. While this approach does not attempt the analytical rigor of a nonlinear dynamic analysis, it was developed through careful evaluation of a modest body of research performed in the centrifuge, small scale shake table, large scale shake table, and full size field tests. Where research results were insufficient to adequately address an issue, opinion of both researchers and industry experts was utilized. Since every project has unique aspects, these guidelines should not be used to constrain or replace engineering judgment. These guidelines present a framework for analysis that should be followed where possible, but with the freedom to extend them as needed to address unique circumstances.

Required Software

These guidelines were developed with the expectation that the reader has access to LPILE 5.0 to perform lateral pile analysis. Many programs are available that perform p-y curve based lateral pile analysis. The somewhat unique and critical feature incorporated in LPILE 5.0 is the ability to impose a free field soil displacement against the pile by adjusting the location of the base of the soil springs. Other codes that offer this capability should be sufficient to implement the recommended procedures. For projects that fall into the Foundation Restrained Displacement design case (defined in Section 2.2) use of a slope stability program will also be necessary. No special functionality will be required so most commercial slope stability programs will be suitable. For the evaluation of pile or shaft moment capacity, LPILE 5 can be used, though use of a program such as X-Section or XTRACT may offer some advantages as will be discussed in Section 2.3.

2 OVERVIEW OF DESIGN PROCEDURE

These guidelines apply an equivalent nonlinear static analysis procedure to two distinct design cases that are depicted in Figure 2.1 and explained in Sections 2.1 and 2.2. Since there are many components to the overall procedure, each involving a spectrum of calculation detail, a single-page overview diagram is provided in Appendix D. This diagram includes references to corresponding document Sections and Tables that provide specific detail. Design examples are provided in Section 4.

The design procedures rely on peak ground acceleration (PGA) and magnitude to characterize the seismic hazard. For Caltrans application this hazard should reflect a 5% in 50 years probability of exceedence.

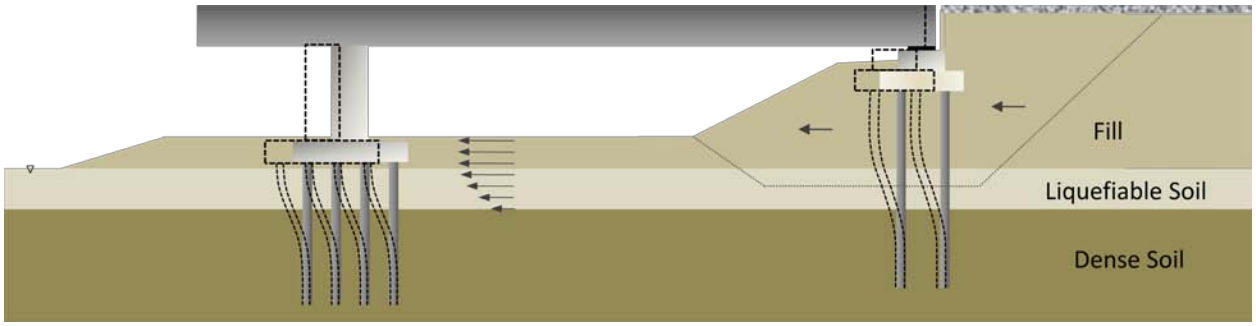

Figure 2.1. Schematic of typical lateral spreading problem. The limited width of the approach fill allows the abutment foundation to partially restrain the movement of the failure mass. The interior bent is subject to a broad failure mass and is unable to restrain the failure mass's movement.

2.1 Unrestrained Ground Displacement Design Case

When the displacing soil mass above and adjacent to the foundation is so large that its movement is unimpeded by the presence of the foundation, the displacement is characterized as "unrestrained". In an unrestrained displacement case the soil beyond the localized failure zone immediately surrounding the foundation displaces the same amount regardless of the presence of the foundation. In Figure 2.1, if one assumes broad transverse continuity of the site conditions, the lateral resistance of the interior bridge bent will be small relative to the overall slide gravity and inertial loads, and thus will fail to significantly restrain the movement of that mass. Key elements of this design case are the estimation of crust displacement and the calculation of the corresponding foundation loads and displacement resulting from the crust movement.

2.2 Foundation Restrained Ground Displacement Design Case

When the displacing soil mass above and along side of the foundation is limited in volume such that movement of this mass is partially restrained by the presence of the foundation, the displacement is characterized as "restrained". The prototypical case is that of an approach embankment acting on abutment piles. Since the displacing soil mass is limited to the dimensions of the approach embankment, the abutment piles, if sufficiently strong and stiff, can act to significantly restrain the down slope movement. Key elements of this design case are evaluating the load-displacement behavior of the pile group, determining the displacement of the sliding mass as a function of the pile group restraining force, and determining the displacement where the foundation resistance is compatible with the slide mass displacement.

2.3 Analytical Framework

The recommended design procedures are based on an equivalent nonlinear static analysis. In these procedures, the foundation is loaded by a laterally displacing soil mass in conjunction with inertial loading from the superstructure, as depicted in Figure 2.2. The interaction between soil and foundation is modeled using nonlinear soil springs (p-y

curves). Liquefied soil is modeled using either factored p-y curves, or by modeling the liquefied layer as a soft clay with undrained shear strength equal to the residual strength of the liquefied soil.

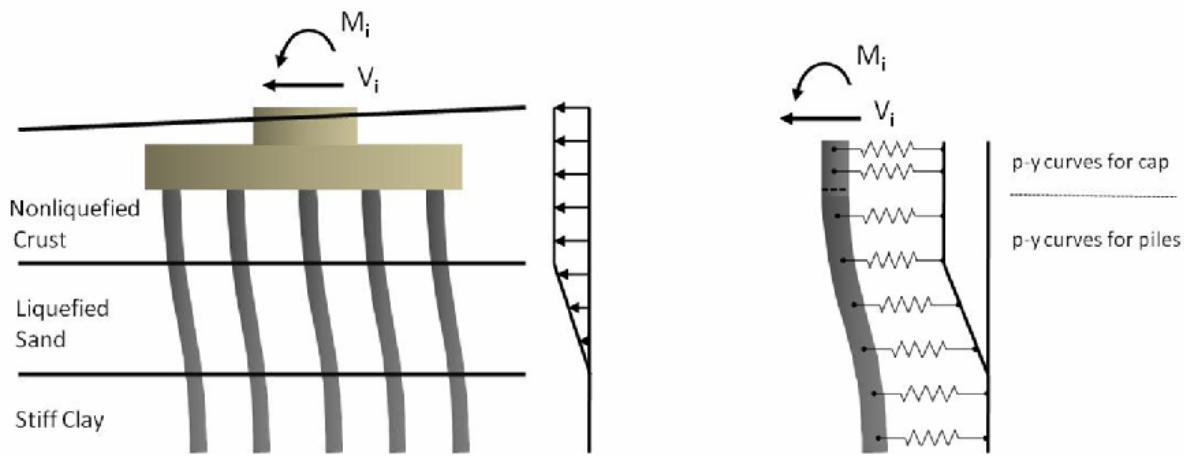

Figure 2.2. The analysis procedure imposes a static soil displacement to push the foundation while it's simultaneously under inertial loading from the superstructure (*left*). The procedure is implemented in LPILE using an equivalent single pile and scaled p-y curves (*right*).

Since LPILE 5.0 has the somewhat unique capability to impose free field soil displacements on a pile model by modifying the base locations of the p-y springs, use of LPILE 5.0 will be assumed for this analysis. LPILE 5.0 is limited to a single pile analysis, however, so an equivalent *superpile* must be specified such that it mimics the behavior of the foundation being analyzed. Table 2.1 summarizes the parameter modifications required in order to achieve equivalence between a pile group and a single *superpile*, assuming linear-elastic pile behavior.

Use of nonlinear pile models

While use of linear-elastic pile models will provided sufficient accuracy in some design cases, use of nonlinear pile models is generally recommended. LPILE 5.0 has a convenient option to specify a nonlinear pile (i.e. it generates a moment –curvature relation), but this option isn't directly applicable to our scaled *superpile*. Since the pile model is nonlinear, one cannot simply scale material or geometry properties to create an equivalent *superpile*. A second issue with LPILE 5.0's nonlinear concrete model is that it is based on unconfined concrete strength. Since Caltrans requires piles and shafts to have significant levels of confinement, the compressive strength of concrete in LPILE 5.0 is typically underestimated by 20 to 30%.

To implement a nonlinear *superpile* in LPILE 5.0, an option for user-specified M-EI (moment –stiffness) curves is used. The following steps are required to generate the desired M-EI curve:

1. Develop a moment curvature curve for a single pile.
2. Scale the moment in the M-ϕ curve by the number of piles in the pile group.
3. Determine the yield curvature, ϕ_y, from the M-ϕ plot as shown in Figure 2.3. Calculate the allowable curvature ϕ_a as $\phi_a = 12\ \phi_y$. Extend the M-ϕ curve to the point (ϕ_a , 1.1 M_{max}).
4. M-EI points are calculated at several points along the curve using the fact that EI = M/ϕ.

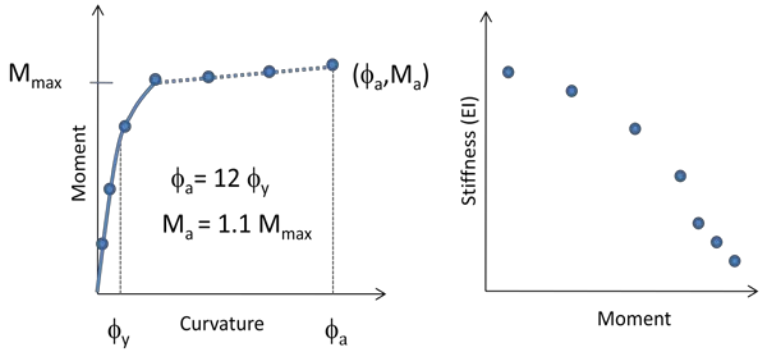

Figure 2.3. Creation of the *superpile* M-ϕ curve for nonlinear analysis. The moment curve shown is the result of multiplying the moments in the single pile M-ϕ curve by the number of piles in the pile group.

TABLE 2.1: Modeling a pile group with an equivalent single linear-elastic pile.

	Group Property	Equivalent Single Pile Property	Notes
Pile Cap			
Length and width	W_L, W_T	B	cap p-y curve is adjusted to account for cap loads
Bending stiffness	Rigid	100nEI *	set large EI to achieve rigidity
Rotational stiffness	K_θ	K_θ	applied as a rotational restraint at the top of the pile
Passive and side resistance		p-y curve	user specified
Piles			
Diameter	B	B	
Bending Stiffness	EI	nEI	
Soil Resistance	p-y curve	p-y curve**	**"p" is multiplied by n and a group reduction factor (GRF)
			* n is the number of piles in the group. Refer to Sec. 3.1 for other parameter definitions.

3 ANALYSIS PROCEDURE

3.1 Calculation of Foundation Loads Due to the Soil Crust

Loads on the foundation due to the down slope movement of the soil crust typically dominate other loads. The interaction between the foundation and soil crust can be modeled using user-specified p-y curves in LPILE 5.0. A trilinear force-deflection model, shown in Figure 3.1, is recommended as the basis for the p-y curves. This model is defined by the parameters F_{ULT} and Δ_{max} which represent the ultimate crust load on the pile cap or composite cap-soil-pile block (see discussion below in *Determination of Critical Failure Surface*) and the relative soil displacement required to achieve F_{ULT}, respectively. The determination of these parameters will be described below. Once the force-displacement relationship is determined, a p-y curve can be defined by dividing the force by the pile cap or composite block thickness.

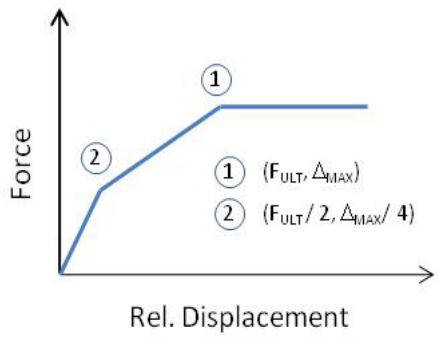

Figure 3.1. Idealized force-deflection behavior of the pile cap. The trilinear curve is defined by the parameters F_{ULT} and Δ_{MAX}.

Definition of Dimension Parameters

A typical foundation configuration and reference dimensions are provided in Figure 3.2. W_L and W_T refer to the longitudinal and transverse pile cap widths, respectively. D is the depth from ground surface to the top of pile cap and T is the pile cap thickness.

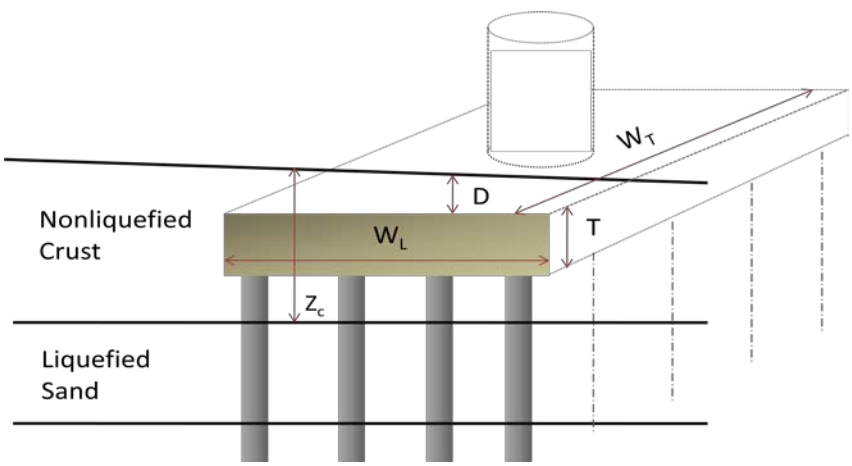

Figure 3.2. Pile foundation schematic with transverse and longitudinal width dimensions W_T and W_L, pile cap thickness T, depth to top of cap D, and crust thickness Z_C.

Determination of F_{ULT}

The maximum crust load on the pile cap can be calculated according to equation (1):

$$F_{ULT} = F_{PASSIVE} + F_{SIDES} \tag{1}$$

In this equation, $F_{PASSIVE}$ refers to the passive force resulting from the compression of soil on the up slope face of the foundation and F_{SIDES} refers to the friction or adhesion of the soil moving along the side of the foundation. Note that a friction force below the pile cap caused by soil flowing through the piles is ignored along with a possible active force on the down slope side of the foundation (acting up slope). These forces are relatively small compared to $F_{PASSIVE}$, act against each other, and are difficult to estimate.

Determination of Critical Failure Surface

In order to determine F_{ULT} we consider two possible failure cases, as shown in Figure 3.3. The case that results in smaller foundation loads is selected for calculation of F_{ULT}. In Case A, a log-spiral based passive pressure is applied to the face of the pile cap. This passive pressure is combined with the lateral resistance provided by the portion of pile length that extends through the crust. A side force on the pile cap is added to the passive resistance.

Case B assumes that the pile cap, soil crust beneath the pile cap, and piles within the crust act as a composite block. This block is loaded by a Rankine passive pressure and side force developed over the full height of the block. Rankine passive pressure is assumed in this case because the weak liquefied layer directly beneath the composite block cannot transfer the stresses required to develop the deeper log-spiral failure surface that is generated by wall face friction.

For most practical problems, Case B will result in smaller foundation loads, though the controlling mechanism is dependent on the size and number of piles, and the thickness of crust. The most accurate way to determine the controlling mechanism is to use LPILE 5.0 to model each case. For design efficiency, however, an approximate calculation of F_{ULT} for each case can be performed to determine the controlling design case. In most instances, one design case will clearly dominate (typically Case B). If $F_{ULT-A} \approx F_{ULT-B}$ then a more complete comparison can be made by modeling both cases in LPILE 5.0..

The estimation of F_{ULT} for Case A and Case B can be performed as follows:

$$F_{ULT-A} \approx F_{PASSIVE-A} + F_{PILES-A} + F_{SIDES-A} \tag{2a}$$

where $F_{PASSIVE-A}$ is given by equation (3), using K_p(log-spiral).

$$F_{PILES-A} \approx n \cdot GRF \cdot P_{ULT} \cdot L_c \tag{2b}$$

where n is the number of piles, GRF is the group reduction factor defined in Section 3.2, P_{ULT} is the ultimate pile resistance determined in Figure 3.4, and L_c is the length of pile extending through the crust. $F_{SIDES-A}$ is given in equation (7a) or (7b).

$$F_{ULT-B} \approx F_{PASSIVE-B} + F_{SIDES-B} \tag{2c}$$

where $F_{PASSIVE-B}$ is given by equation (3), using K_p(Rankine). $F_{SIDES-B}$ is given in equation (7a) or (7b) but with cap thickness T replaced by the thickness of the composite block ($Z_c - D$ in Figure 3.2).

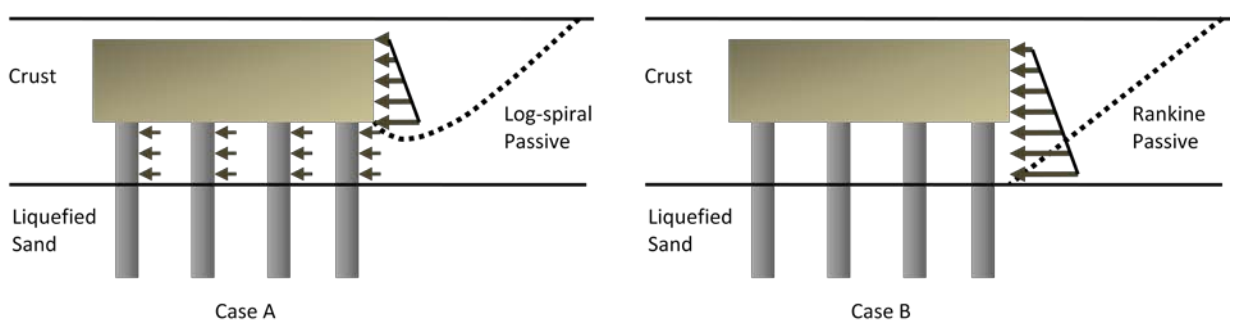

Figure 3.3. Two possible design cases for the calculation of the ultimate passive load due to the soil crust. Case A considers the combined loading of a log-spiral passive wedge acting on the pile cap and the ultimate resistance provided by the portion of

individual pile length above the liquefied zone. Case B considers the loading of a Rankine passive wedge acting on a composite soil block above the liquefaction zone.

Estimation of P_{ULT}

For SAND:

$$P_{ULT} = (C_1 \overline{H} + C_2 B)\gamma \overline{H}$$

For CLAY:

$$P_{ULT} = 9\, c\, B$$

Where: P_{ULT} = ultimate lateral resisting force per unit length of pile
$\overline{H}$ = average pile depth in the crust
B = pile diameter
γ = effective unit weight of the crust
$C_1 = 3.42 - 0.295\,\phi + 0.00819\,\phi^2$
$C_2 = 0.99 - 0.0294\,\phi + 0.00289\,\phi^2$
ϕ = friction angle of crust $\quad 20 \le \phi \le 40$
c = undrained shear strength

Figure 3.4. Calculation of P_{ULT} for Sands and Clays, approximated from formulations by API (1993).

$F_{PASSIVE}$ (c-ϕ soils)

For soils with a frictional component, $F_{PASSIVE}$ can be estimated using equation (3).

$$F_{PASSIVE} = \left(\overline{\sigma_v'} K_p + 2c'\sqrt{K_p}\right)(T)(W_T)(k_w) \tag{3}$$

In equation (3) $\overline{\sigma_v'}$ is the mean vertical effective stress along the pile cap face, K_p is the passive pressure coefficient, $c'$is the cohesion intercept, and k_w is an adjustment factor for a wedge shaped failure surface. In general, for cohesionless soil K_p should be based on a log-spiral failure surface. A convenient approximation for K_p (log-spiral) is given in equation (4), where ϕ is the peak friction angle of the crust, and δ is the pile cap-soil interface friction angle (recommended as $\phi/3$ for cases of liquefaction).

$$K_p\ (log\text{-}spiral) = \begin{cases} Tan^2\left(45 + \frac{\phi}{2}\right)\left(1 + (0.8152 - 0.0545\,\phi + 0.001771\,\phi^2)\frac{\delta}{\phi} - 0.15\left(\frac{\delta}{\phi}\right)^2\right) & \phi > 0 \\ 1 & \phi = 0 \end{cases} \tag{4}$$

When ϕ is >0, the approximation is valid for ϕ ranging from 20° to 45° and $\delta \le \phi$.

For cases where the pile cap or composite cap-pile-soil block (case B) extends to the top of the liquefiable layer, K_p should be calculated using Rankine's formulation, equation (5), instead of a log-spiral solution since the presence of the liquefiable layer impedes the development of the deeper log-spiral failure surface.

$$K_p(Rankine) = Tan^2(45 + \frac{\varphi}{2}) \tag{5}$$

A solution for k_w, developed by Ovesen (1964), is given in equation (6).

$$k_w = 1 + \left(K_p - K_a\right)^{\frac{2}{3}}\left(1.1\left(1 - \frac{T}{D+T}\right)^4 + \frac{1.6}{1+\frac{5W}{T}} + \frac{0.4\left(K_p - K_a\right)\left(1 - \frac{T}{D+T}\right)^3}{1+\frac{0.05W}{T}}\right) \quad (6)$$

$F_{PASSIVE}$ (c-only soils)

For cases where the crust is entirely cohesive (no frictional strength component) $F_{PASSIVE}$ should be estimated using equation (7) (Mokwa et al., 2000)

$$F_{PASSIVE} = \left(4 + \frac{\gamma(D+T)}{c} + \frac{D+T}{4\,W_T} + 2\alpha\right) c\, W_T \frac{(D+T)}{2} \quad (7)$$

In equation (7) α is an adhesion factor and can be assumed to be 0.5.

F_{SIDES}

F_{SIDES} can be calculated using equation (8a) for effective stress conditions and equation (8b) for total stress conditions. In both instances, α is an adhesion factor assumed to be 0.5. All other variables are defined as in equations (3) and (4).

$$F_{SIDES} = 2\left(\overline{\sigma_v'}\, Tan(\delta) + \alpha c'\right) W_L T \quad (8a)$$

$$F_{SIDES} = 2\,\alpha c\, W_L \mathrm{T} \quad (8b)$$

<u>Determination of ΔMAX</u>

Traditionally, passive resistance against a rigid wall will take 1 to 5% of the wall height to fully mobilize. Empirical observation and theoretical studies by Brandenberg (2007) suggest that for the case of a crust overlying a liquefied layer, mobilization of the full passive force may require relative displacements much larger than 5% of wall height. This larger deformation stems from the greatly reduced capacity of the underlying liquefied soil to transmit shear stress from the bottom of the crust. These stresses are thus constrained to spread horizontally (instead of downward) and spread large distances through the crust. This effect is most pronounced when the crust thickness is equal to or smaller than the pile cap thickness and the pile cap width is large relative to the crust thickness. The effect diminishes as the crust becomes thicker relative to both the pile cap thickness and width. This behavior is accounted for in equation (9a) by using the adjustment factors f_{depth} and f_{width}. These factors are given in equation (9b) and (9c) and shown graphically in Figure 3.5. Refer to Figure 3.2 for parameter definitions used in equations (9a) - (9c).

$$\Delta_{MAX} = (T)\left(0.05 + 0.45\, f_{depth} f_{width}\right) \quad (9a)$$

$$f_{depth} = e^{-3\left(\frac{Z_c - D}{T} - 1\right)} \quad (9b)$$

$$f_{width} = \frac{1}{\left(\frac{10}{\frac{W_T}{T}+4}\right)^4 + 1} \quad (9c)$$

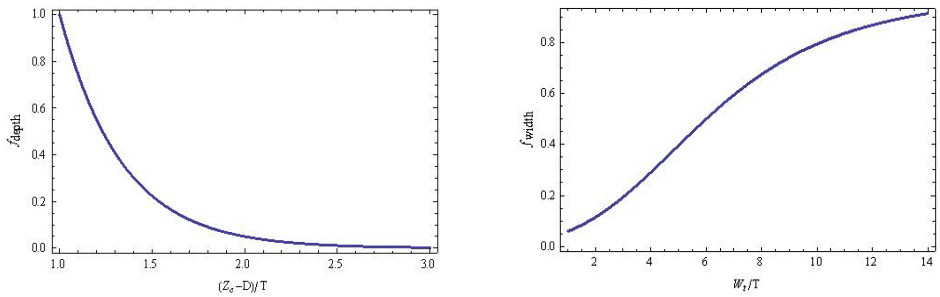

Figure 3.5. f_{depth} as a function of the ratio of crust thickness to pile cap thickness (left). f_{width} as a function of the ratio of pile cap width to pile cap thickness (right). (Brandenberg, personal communication)

3.2 Calculation of p - y Curves for Piles

As discussed in Section 2.3, since LPILE 5.0 is limited to a single pile analysis, an equivalent *superpile* must be specified. In order to correctly model the soil resistance acting on the *superpile*, the "p" in the p-y curves for a single group pile must be scaled by a factor equal to the number of group piles multiplied by an adjustment factor for group efficiency, or Group Reduction Factor (GRF), as given in equation (10).

$$p_{super} = p_{single} \cdot n \cdot GRF \tag{10}$$

The p-y models implemented in LPILE 5.0 are based on Matlock (1970) (soft clay), Reese et al. (1975) (stiff clay), and Reese et al. (1974) (Sand). LPILE 5.0 also allows the user to input p-y curves directly, as will be required for the modeling of the pile cap.

<u>Group Reduction Factors</u>

Piles in groups tend to be less efficient in resisting lateral load, on a per pile basis, than isolated piles. This lost efficiency is caused by the overlapping stress fields of closely spaced piles. Leading row piles tend to attract more load than trailing rows, for example, which tend to be shielded by the rows in front of them. In order to match group behavior with a single pile, a composite group efficiency factor, or Group Reduction Factor (GRF), must be applied to the individual p-y curve as a p-multiplier. Figure 3.6 presents p-multipliers recommended by Mokwa (2000) as a function of pile spacing and transverse oriented row. In order to determine the GRF, the factor for each row should be averaged. For example, a 5 row pile group with 3 diameter spacing would have a GRF = (0.82 + 0.67 + 0.58 + 0.52 + 0.52) / 5 = 0.62.

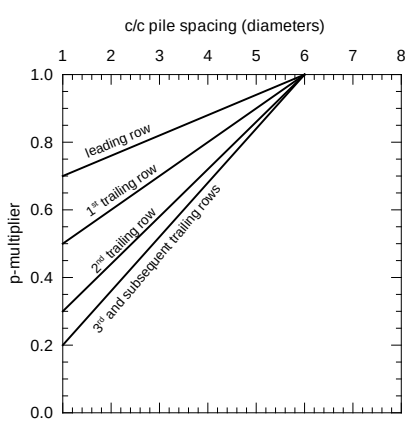

Figure 3.6. Recommended p-multiplier for group effects (from Mokwa, 2000)

p-y Curves for Liquefied Soil

P-Multiplier (m_p) Method

The dramatic strength loss associated with liquefaction can be accounted for through application of p-multipliers that scale down p-y curves reflective of the nonliquefied case. Figure 3.7 shows the range of back calculated p-multipliers (Ashford et al. 2008) from a number of studies. A recommended equation for m_p is also given and plotted against the back calculated values. In the equation, N refers to the clean sand equivalent corrected blow count $(N_1)_{60CS}$. A clean sand correction by Idriss and Boulanger (2008) is provided in Appendix C. The recommended p-multiplier equation in Figure 3.7 is appropriate for soils that reach 100% excess pore pressure ratio. In soils that are not expected to fully liquefy but will reach a pore pressure ratio significantly greater than zero, m_p can be scaled proportionately by 100 / r_u where r_u is the excess pore pressure ratio (percent).

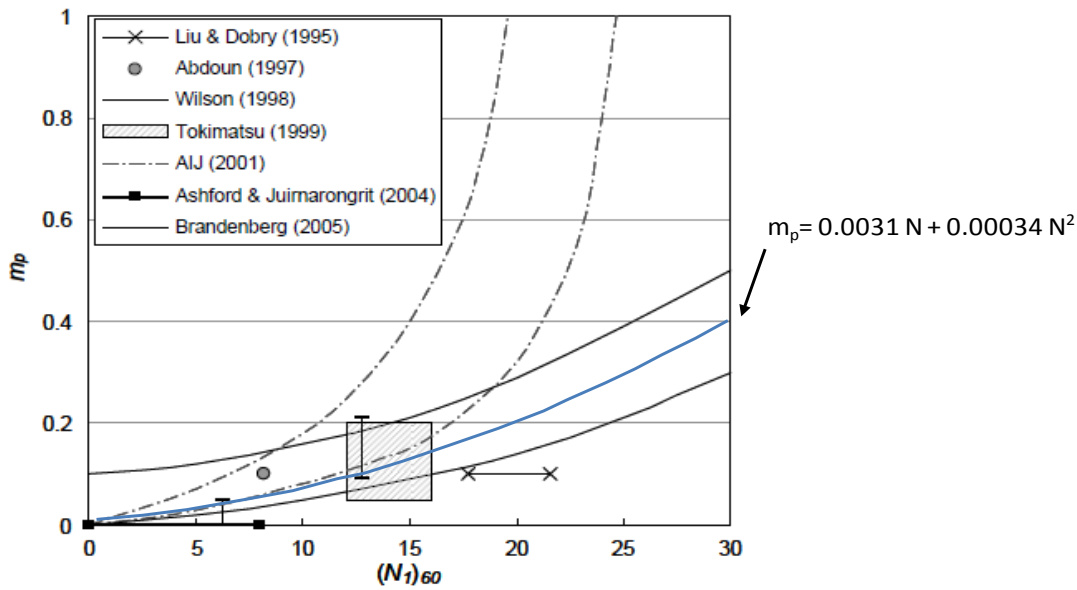

Figure 3.7. p-multiplier (m_p) vs. clean sand equivalent corrected blow count, $(N_1)_{60CS}$, from a variety of studies. An equation is given for the recommended design curve.

Residual Strength Method

An alternative to the p-multiplier method is to develop p-y curves based on soft clay p-y models (e.g. Matlock 1974) where the residual strength of the liquefied soil is used in place of the undrained shear strength of the soft clay. Residual strength can be estimated using the following relation by Kramer and Wang (2007):

$$S_r = 2116 \cdot \exp\left(-8.444 + 0.109\,(N_1)_{60} + 5.379\left(\frac{\sigma_v'}{2116}\right)^{0.1}\right) \tag{11}$$

In equation (11) both S_r and σ_v' are in units of psf. The SPT blow count in this relation does not require adjustment for fines content. It is recommended that ε_{50} = 0.05 be used when applying the Matlock soft clay procedure.

Modification to p-y Curves Near Liquefaction Boundary

The occurrence of liquefaction will affect the potential lateral resistance of nonliquefied layers directly above or below the liquefied strata. p-multipliers can be used to reduce the subgrade reaction of nonliquefied soils in the vicinity of a liquefied layer as shown in Figure 3.8.

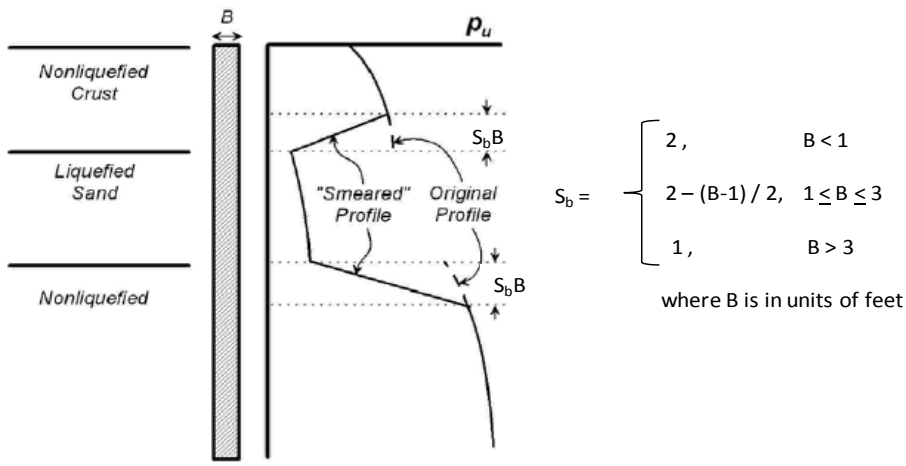

Figure 3.8. Modification to the ultimate subgrade reaction, p_u, to account for the weakening effect the liquefied sand exerts on overlying and underlying nonliquefied strata.

If z is the distance (in feet) above or below the liquefaction boundary and $p_{u\text{-}L}$ and $p_{u\text{-}NL}$are the ultimate subgrade reactions in the adjoining liquefied and nonliquefied layers, respectively, then a p-multipier (m_p) should be applied as given in equation (12). This p-multiplier should be applied at increasing distance from the liquefaction boundary until it equals 1.

$$m_p = \frac{p_{u-L}}{p_{u-NL}} + \left(1 - \frac{p_{u-L}}{p_{u-NL}}\right)\left(\frac{z}{s_b B}\right) \tag{12}$$

3.3 Determination of Rotational Stiffness K_θ

Estimation of the rotational stiffness of a pile group can be simplified by assuming that the axial stiffness of a pile is the same in uplift and compression. If this assumption is true, or approximately true, the foundation will rotate about its center and the rotational stiffness can be estimated as shown in Figure 3.9. If the axial stiffness of the pile is considerably larger in compression (due to large end bearing) then the rotational stiffness of the pile group is best estimated using a pile group analysis program (e.g. GROUP). K_{ax} can be estimated by assuming that 75% of the ultimate pile capacity is achieved at 0.25-inch axial displacement. For the case of a Class 100 pile, this corresponds to K_{ax} = 0.75 (400 kips) / 0.25 in = 1200 kips/in.

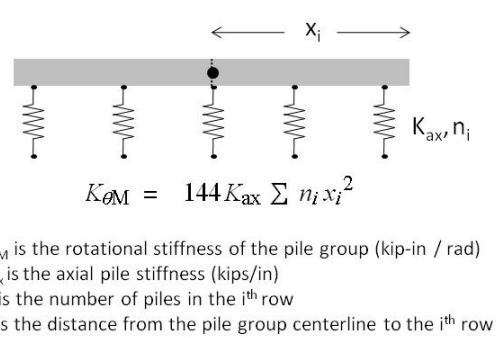

Figure 3.9 Calculation of rotational stiffness of the pile group. The method assumes that the single pile compressive stiffness is approximately equal to the uplift stiffness.

3.4 Combination of Kinematic and Inertial Loads

Back analysis of ground failure occurrences as well as eyewitness accounts indicate that large ground displacements can occur both during and after strong shaking, the latter caused by redistribution of pore pressures. To predict whether the spreading is likely to occur during or after shaking would generally require a level of site characterization and analysis beyond most project budgets. For this reason, it is assumed here that lateral spreading will occur during strong shaking and that inertial loading of the foundation must be considered in tandem with kinematic loading.

<u>Typical Bridge Bent Case</u>

Foundation load demand includes inertial forces from the superstructure and pile cap and kinematic loads from the soil crust pushing into the pile cap. The dynamic interaction of these forces is complex and is affected to varying degrees by the changing nature of the ground motion and foundation stiffness as liquefaction initiates. Also significant are the changing dynamic characteristics of the superstructure as the bridge column(s) undergoes significant yielding under strong shaking.

When combining kinematic and inertial loads in an equivalent static analysis, one must account for the fact that individual peaks of the contributing dynamic loads and kinematic demands generally occur at different times. Back analysis of centrifuge experiments and numerical simulations demonstrate that peak demands can be estimated reasonably well using equations (13a and 13b).

$$100\%\ (kinematic) + 50\%\ (inertial) \rightarrow (peak\ pile\ cap\ disp) \tag{13a}$$

$$100\%\ (kinematic) \pm 50\%\ (inertial) \rightarrow (peak\ pile\ moment\ or\ shear) \tag{13b}$$

Note that in some instances peak pile demands occur when the direction of the inertial loading is opposite to the kinematic loading.

Estimation of Inertial Loads

Superstructure

For most design cases the bridge column is expected to yield. In this case the peak inertial load due to the superstructure can be calculated as shown in Figure 3.10.

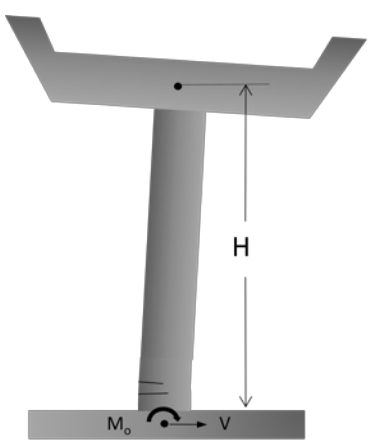

	Single col. trans.	Single col. long.	Multi-col.
Top fixity	Free	Fixed	Fixed
Bottom fixity	Fixed	Fixed	Free
Inertial mom.	M_o	M_o	0
Inertial shear	$\frac{M_o}{H}$	$\frac{2M_o}{H}$	$\frac{M_o}{H}$

Figure 3.10. Calculation of inertial shear demand for the case of a yielding column. M_o refers to the overstrength moment and can be assumed to be 1.2 x plastic column moment.

If the column is not expected to reach its moment capacity then superstructure inertial force and moment can be estimated according to equations (14a) and (14b), where m_{trib} refers to the tributary mass of the superstructure and $S_a(T_1)$ refers to the spectral acceleration at the first mode period. H and column rotational constraints are as shown in Figure 3.10.

$$V_i = m_{trib} \cdot S_a(T_1) \tag{14a}$$

$$M_i = V_i \cdot H \qquad (free - fixed) \tag{14b}$$

$$M_i = \frac{V_i \cdot H}{2} \qquad (fixed - fixed)$$

Pile cap

The inertial force resulting from the pile cap can be estimated using equation (15), where the peak ground

$$F_{CAP_i} = 0.65 \cdot PGA_{No\ Liq} \cdot m_{cap} \tag{15}$$

acceleration (PGA) corresponds to the non-liquefaction case and m_{cap} refers to the mass of the pile cap. The 0.65 factor represents a reduction in PGA resulting from the onset of liquefaction.

Abutments

In the case of a pedestal or seat type abutment, the superstructure is separated from the supporting abutment foundation by bearings. Because these bearing are free to rotate, no moment demand is transmitted to the abutment foundation by the superstructure. Furthermore, the superstructure is free to translate longitudinally until the abutment backwall is engaged (typically after about 1-inch displacement). Though some inertial load may be transferred to the abutment foundation through the backwall, the backwall is generally designed as a weak fuse with only modest capacity to transfer load. Thus, it is recommended that for the case of seat type abutments, inertial forces should be ignored.

3.5 Estimating Crust Displacements

The displacement of the ground surface resulting from liquefaction can be highly variable and depends upon local topography, soil stratigraphy, material properties, and ground motion. Simplified displacement estimation procedures have been developed by many authors, all sharing relatively large uncertainty. Two methods are recommended here. Where the failure surface is somewhat predictable, for example in the case of an abutment as shown in Figure 3.11 (right), a Newmark based estimation procedure is preferred. The Bray and Travasarou (2007) procedure is recommended to implement the Newmark approach. Where the ground surface is a gentle slope, ground displacement is typically the result of distributed shear and a strain potential based approach is preferred. The procedure by Faris (2006) is recommended for strain potential based estimates.

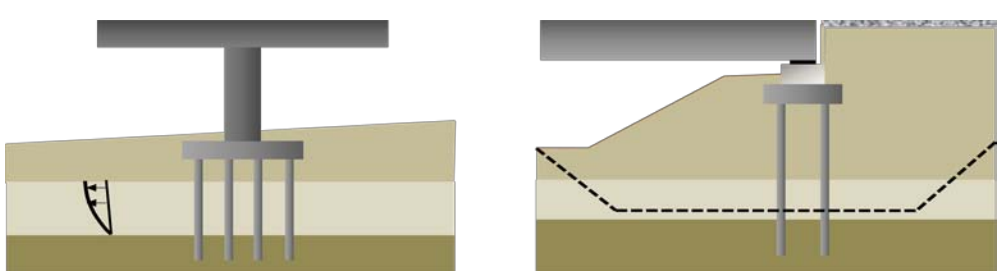

Figure 3.11. (Left) Typical profile where failure surface is unpredictable and a strain potential based procedure is recommended. (Right) Failure surface is reasonably predictable and a Newmark based procedure is recommended.

Estimating Displacements using Bray and Travasarou (2007)

In general, Newmark type procedures model slope displacements as a rigid block sliding on a planar surface. The shear strength of the material immediately below the sliding block (assumed to be constant) and the steepness of the slope define the block's propensity to slide downhill. This propensity is characterized by the system's yield coefficient k_y. When the horizontal acceleration due to earthquake shaking exceeds k_y, the block breaks free from the underlying slope and moves downhill until the block velocity and slope velocity again become equal. This model can be extended to non-planar failure surfaces by using slope stability analysis to determine k_y by finding the horizontal acceleration required to achieve a factor of safety of unity. In this calculation, the strength of the liquefiable zone can be estimated using equation (11).

Bray and Travasarou (2007) is a regression model for slope displacement developed by running large suites of earthquake records through a nonlinear deformable sliding block model. Their regression model considers the affect of the dynamic response of the sliding mass by using spectral acceleration at the fundamental period of the sliding mass as an input parameter. Their model was not developed considering the affects of liquefaction, however. For application here, it is recommended that the sliding mass be considered rigid and that peak ground acceleration (PGA) be used as the ground motion input parameter. The recommended form of the Bray and Travasarou model is given in equation (16). In equation (16) M_w is the magnitude of the design event. As noted in Section 2, the PGA and magnitude should reflect a 5% in 50 year hazard level.

$$D(cm) = Exp[-0.22 - 2.83\, Ln(k_y) - 0.333\, Ln(k_y)^2 + 0.566\, Ln(k_y) Log(PGA) + 3.04\, Ln(PGA) - 0.244\, Ln(PGA)^2 + 0.278\, (M_w - 7)] \quad (16)$$

Estimating Displacements using Faris et al. (2006)

The procedure by Faris (2006) relies on the Displacement Potential Index (DPI) which is defined as the integration of potential shear strains within a liquefiable layer (or across multiple layers if they exist) over the thickness of the layer(s). In equation form,

$$DPI = \int_{\substack{liq.\\layer}} \gamma_{max}\, dz \quad (17)$$

As implemented here, a liquefiable layer is considered to be any layer with a factor of safety for liquefaction triggering $\leq$ 1.10. The limiting shear strain γ_{max} can be estimated using Figure 3.12. For computational convenience, a routine that approximates Figure 3.12 is given in Appendix A.

Since Figure 3.12 is based on a clean sand equivalent SPT blow count, an adjustment is required to account for the presence of fines. Faris (2006) recommends the fines adjustment shown in Figure 3.13. This adjustment is given in formula form in Appendix B. Note that this adjustment reflects the influence of non-plastic fines on strain potential and is not suitable for triggering assessment.

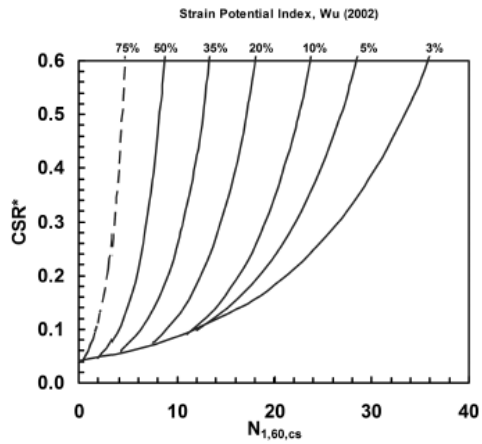

Figure 3.12. Strain Potential Index (γ_{max}) by Wu (2002). CSR* refers to the magnitude corrected cyclic stress ratio. Magnitude correction is given in Seed et al. (2003). Correction by Idriss and Boulanger (2004) is sufficiently close to that of Seed and is given by $MSF = 6.9 \exp\left(\frac{-M}{4}\right) - 0.058 \leq 1.8$.

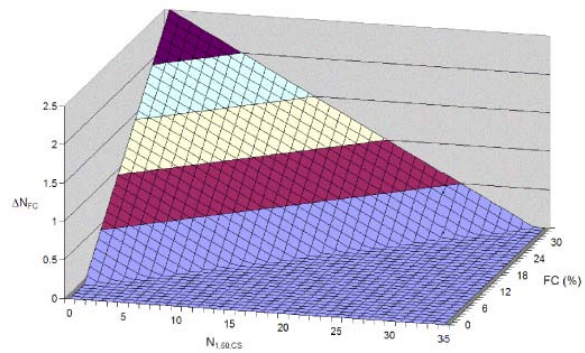

Figure 3.13. Recommended adjustment for non-plastic fines from Faris (2006). FC is the percent passing the No. 200 sieve. A numerical version of the adjustment is given in Appendix B.

Once DPI is calculated using equation (17), the horizontal slope displacement can be estimated using the Simplified Maximum Displacement model from Faris (2004) given in equation (18). Note that equation (18) is valid only for units of meters.

$$H(m)_{max} = DPI(m)^{1.07} \tag{18}$$

It has generally been observed that ground displacement near an open face is larger than at locations further from the face. To account for this effect, not directly accounted for in Faris's simplified model, an amplification factor based on Zhang (2004) is applied to H_{max} as shown in Figure 3.14.

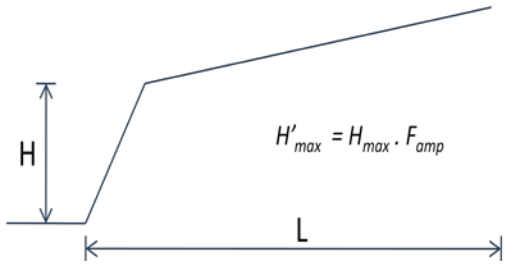

$$F_{amp} = \begin{cases} 2 & for \quad L/H < 4 \\ 6\,(L/H)^{-0.8} & for \quad 4 < L/H < 9 \\ 1 & for \quad 9 < L/H \end{cases}$$

Figure 3.12. Modification of H_{max} to account for open slope face conditions. From Zhang (2004).

For locations near the face, the static factor of safety (FS) should be evaluated using residual strength per equation (11). If the location falls within a failure surface with a FS $\leq$ 1.05, then the horizontal crust displacement should be assumed to be equal to the face height H. For nearly flat locations (slope < 1%) without a nearby open face, equation (18) can be modified to introduce linear slope dependence.

$$H_{max} = S \cdot DPI^{1.07} \quad for\ 0.25 \leq S < 1\ and\ S\ is\ the\ slope\ (\%) \tag{19}$$

For locations with a flatter slope than 0.25%, a minimum S of 0.25 should be used.

3.6 Unrestrained Crust Displacement Case Procedures

As discussed in Section 2.1, when the driving force of the sliding mass is much larger than the potential resistance of the foundation, the crust displacement is considered to be "unrestrained" and its displacement estimate is performed without regard to the presence of the foundation. The following outlines the various steps required to perform a foundation assessment for the case of unrestrained soil displacement. A worked example problem is provided in Section 4.1.

1) Assess the soil profiles liquefaction potential using peak ground acceleration (PGA) based on the 5% in 50 years hazard. The liquefaction assessment should be based on procedures outlined in Youd et al. (2001).
2) Assign residual strengths to liquefiable layers using equation (11).
3) Evaluate the slope factor of safety (FS). If FS$\leq$ 1.05 , a flow type failure with corresponding large displacement should be assumed. So long as the displacement value is sufficient to fully mobilize the ultimate passive force of the crust, the analysis is insensitive to specific displacement assumptions. Typically, an assumption of approximately 5 feet is sufficient. If FS > 1.05, determine the crustal displacement using either Faris (2006) or Bray and Travasarou (2007) as outlined in Section 3.5.
4) Develop a foundation model using an equivalent *superpile* per Table 2.1, pile cap p-y curves per Section 3.1, liquefied p-y curves per Section 3.2, and pile rotational stiffness per Section 3.3.
5) Impose on the foundation model a soil displacement profile per Figure 2.2 and Step 3, above. Apply inertial loads in combination with displacement profile per Section 3.4. Evaluate foundation adequacy by comparing calculated demands with the allowable demands given in Table 3.1 (Section 3.8).

3.7 Foundation Restrained Crust Displacement Case Procedures

As discussed in Section 2.2, when the potential sliding mass is limited in size, the lateral stiffness of the foundation can impede its movement. Consideration of this restraining effect can result in significant economy since reduced displacement demand results in improved foundation performance. Accounting for a foundation's "pinning" effect is not a new concept. Procedures to establish compatible slope and foundation displacements are presented in NCHRP 472, for example. The NCHRP 472 methodology is generally adhered to here, but with minor modification motivated by back analysis of experimental tests.

The following outlines the various steps required to perform a foundation assessment for the case of foundation restrained soil displacement. A worked example problem is provided in Section 4.2.

1) Assess the soil profiles liquefaction potential using peak ground acceleration (PGA) based on a 5% in 50 years hazard. The liquefaction assessment should be based on procedures outlined in Youd et al. (2001)

2) Assign residual strengths to liquefiable layers using equation (11).

3) Develop a foundation model using an equivalent *superpile* per Table 2.1, pile cap p-y curves per Section 3.1, liquefied p-y curves per Section 3.2, and pile rotational stiffness per Section 3.3.

4) Using LPILE 5.0, impose a series of increasing soil displacement profiles on the foundation model. Each displacement increment should be combined with the inertial loads calculated per Section 3.4 (assumed to be zero for the case of abutments). Plot the imposed crustal displacement against the shear force in the *superpile* developed at the center of the liquefiable layer ($\vec{\boldsymbol{R}}$ in Figure 3.16). A typical result is plotted in Figure 3.17 as curve (2).

5) If the bridge deck can be expected to provide longitudinal resistance to abutment movement, calculate the passive force (F_{DECK} in Figure 3.14) expected from full mobilization of this resistance.

6) Perform a slope stability analysis to determine the yield coefficient k_y for a range of possible foundation restoring forces (shown as vector R in Figure 3.16). In this analysis F_{DECK} should be applied as a constant restoring force. The slope stability analysis should constrain the failure surface to the center of the liquefiable layer. Also, there is a tendency for the failure mass to grow larger and larger under increasing levels of horizontal acceleration. It is recommended that this failure surface not extend a distance beyond 4H, where H is the height of the abutment.

7) Since R is determined on a per unit width basis in the slope stability analysis, it needs to be multiplied by the width of the sliding mass. For embankments, a tributary width can be used to account for nonrectangular shape, as shown in Figure 3.15.

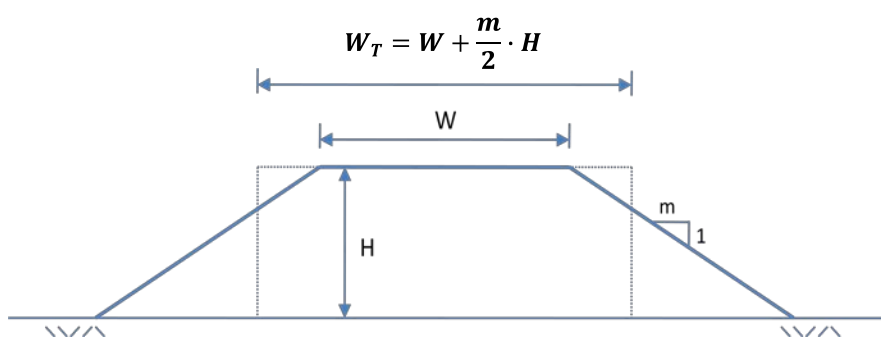

Figure 3.15: Determination of the tributary width of an embankment

8) For each value of k_y calculated in Step 6, use Bray and Travasarou (equation 16) to estimate a corresponding displacement. Plot these displacements as a function of resistance force **R** (curve (1) in Figure 3.17).

9) In Figure 3.17, curve (2) reflects the foundation resistive force corresponding to a given crustal displacement. Curve (1) corresponds to the expected crustal displacement given a *constant* resistive force. Note that as the failure mass begins to slide, the foundation resistive force is not constant but increases from zero to the value given by curve (2). Thus, to ensure displacement compatibility between the sliding mass and the foundation resisting its movement, the *average* foundation resisting force must be used. This can be achieved by modifying curve (2) by plotting the average resistance corresponding to a given displacement. Since curve (2) is generally not a straight line, the average needs to be calculated as a "running average". This running average curve is shown in Figure 3.17 as curve (3).

10) The displacement corresponding to the intersection of curves (1) and (3) represents the expected displacement demand on the foundation. To evaluate the adequacy of the foundation, this demand is compared against allowable displacements given in Table 3.1 (Section 3.8). Pile moments and shears at this displacement demand are also compared to the allowable values given in Table 3.1. These demands

should be calculated using inertial loads (if any) in combination with imposed soil displacement demands per Section 3.4.

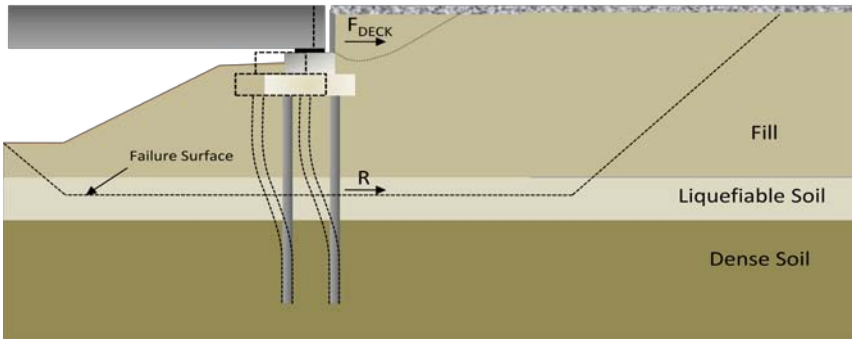

Figure 3.16 A slope stability analysis is performed to determine k_y for a range of foundation resistance values R

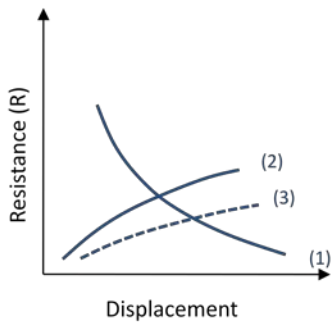

Figure 3.17. Determination of compatible displacements.

3.8 Foundation Performance Criteria

Allowable foundation demands are provided in Table 3.1. A limit on foundation displacement is the primary safety criterion. A foundation displacement of H/20 is seen as damaging but not catastrophic to a structure. If a foundation consists of lightly reinforced elements with very limited ductile capacity, all but small foundation displacements should trigger retrofit or liquefaction mitigation.

Table 3.1: Allowable Foundation Demands

	Cap Displacement	Pile Moment	Pile Shear
Well confined pilings	H/20	$1.0 \cdot M_a(per\ Section\ 2.3)$	SDC 3.6
Well confined abutment pilings	12 inches	$1.0 \cdot M_a(per\ Section\ 2.3)$	SDC 3.6
Poorly confined pilings	2 inches	-	-
*H = column height			

4.0 WORKED EXAMPLES

4.1 Unrestrained Soil Displacement

Problem description

The example concerns the evaluation of a rectangular footing containing sixteen 24-inch diameter CISS piles. The foundation is located on a 2% slope and supports a single 20-foot tall column, 5-feet in diameter, with an overstrength moment capacity of 12,000 k-ft. The column and superstructure form a monolithic connection which is free to rotate under transverse loading. The column and superstructure together weigh 1600 kips. The lateral spreading is assumed to move in a direction transverse to the bridge alignment. The soil profile is shown in Figure 4.1 and the pile layout is shown in Figure 4.2. The 5% in 50 year seismic load corresponds to a magnitude 7.5 event generating both PGA and $S_a(1s)$ of 0.5g.

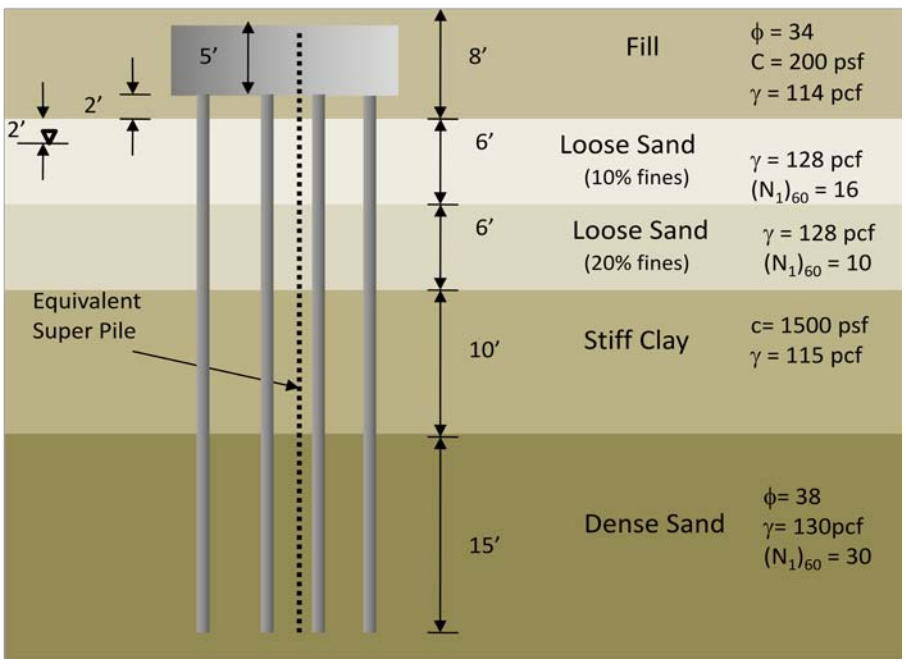

Figure 4.1. Soil profile and properties

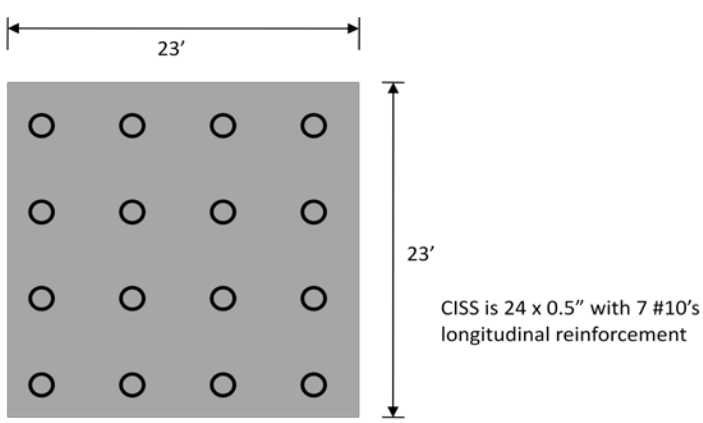

Figure 4.2. Pile layout

Problem solution

We assume that the dimensions of the slope are large and that the foundation itself won't affect the global movement of soil down slope. Thus, we consider the unrestrained crust displacement design case and apply the calculation steps itemized in Section 3.6.

Step 1: Assess liquefaction potential of each layer.

Two zone are considered, the upper loose sand layer with $N_{1,60}$ =16 and the lower loose sand layer with $N_{1,60}$ =10. Following Youd (2001), the cyclic resistance ratio, CRR, is calculated as

$$CRR = CRR_{\sigma_v'=1,\alpha=0} \cdot K_\sigma \cdot K_\alpha$$

For this example problem, K_σ and K_α =1 and $CRR_{\sigma_v'=1,\alpha=0}$ is estimated to be 0.13g for the case of $N_{1,60}$ = 10 (FC=20%) and 0.17g for $N_{1,60}$ = 16 (FC=10%)

The cyclic stress ratio, CSR, is estimated as

$$CSR = 0.65\ \frac{\sigma_v}{\sigma_v'} \frac{A_{max}}{g} r_d$$

For the upper and lower zones we calculate the following (at the center of each zone):

$$CSR = 0.65\ \frac{1296\ psf}{1234\ psf} \cdot 0.5 \cdot 0.98 = 0.33 \qquad CSR = 0.65\ \frac{2064\ psf}{1627\ psf} \cdot 0.5 \cdot 0.96 = 0.40$$

Thus, the factor of safety against liquefaction triggering for both the upper and lower zones are

$$FS_{liq} = \frac{CRR}{CSR} = \frac{0.17}{0.33} = 0.52 \qquad FS_{liq} = \frac{CRR}{CSR} = \frac{0.13}{0.40} = 0.33$$

Since FS_{liq} <1 in both the upper and lower portions of the loose sand layer, both zones are susceptible to liquefaction for the design loading.

Step 2: Estimate residual strengths of the liquefiable zones per Section 3.2.

Using Kramer and Wang (2010), equation (11), we get the following:

Upper zone ($(N_1)_{60}$= 16) S_r = 425 psf

Lower zone ($(N_1)_{60}$= 10) S_r = 255 psf

Step 3: Evaluate slope deformation

Since the slope is only 2%, the FS>1.05. In the case of gentle slopes, the strain potential approach is generally preferred over the Newmark method. Since both the upper and lower portions of the loose sand layer contain fines, we use Figure 3.13 or Appendix B to determine whether a fines correction is necessary. For these cases a fines adjustment is not needed.

To determine γ_{Max} for the upper and lower zones of liquefaction we refer to Figure 3.12. For the upper zone, with a CSR of 0.33 and $N_{1,60cs}$ of 16, we get γ_{Max} = 0.18. For the lower zone with CSR of 0.40 and $N_{1,60cs}$ of 10, we get γ_{Max} = 0.42. DPI is calculated using equation (17):

$$DPI = (0.42)(72\ in) + (0.18)(48\ \text{in}) = 39\ in$$

Using equation (18), we estimate the crust displacement as

$$D = \left(\frac{39\ in}{39.4\ {}^{in}/_{m}}\right)^{1.07} = 1\ m = 39\ in$$

Of the 39 inches of displacement, 30 inches is distributed (linearly) across the lower liquefaction zone and 9 inches is distributed across the upper zone.

Step 4: Develop LPILE 5.0 model

p-y curves for the pile cap

Per Section 3.1, the ultimate crust load, F_{ULT}, must be evaluated for the two design cases shown in Figure 3.3.

Case A:

From equation (2a) we get:

$$F_{ULT-A} \approx F_{PASSIVE-A} + F_{PILES-A} + F_{SIDES-A}$$

Starting with the passive load contribution:

$$F_{PASSIVE-A} = \left(\overline{\sigma_v'}K_p + 2c'\sqrt{K_p}\right)(T)(W_T)(k_w)$$

The various terms can be calculated as follows:

$$K_p = Tan^2\left(45 + \frac{34}{2}\right)\left(1 + (0.8152 - 0.0545 \cdot 34 + 0.001771 \cdot 34^2)\frac{12}{34} - 0.15\left(\frac{12}{34}\right)^2\right) = 4.73$$

$$K_a = Tan^2\left(45 - \frac{34}{2}\right) = 0.28$$

$$\overline{\sigma_v}' = 3.5\ ft \cdot 114\ {}^{lb}/_{ft^3} = 400\ psf$$

$$k_w = 1 + (4.73 - 0.28)^{\frac{2}{3}}\left(1.1\left(1 - \frac{5}{6}\right)^4 + \frac{1.6}{1 + \frac{5 \cdot 23}{5}} + \frac{0.4(4.73 - 0.28)\left(1 - \frac{5}{6}\right)^3}{1 + \frac{0.05 \cdot 23}{5}}\right) = 1.20$$

Putting this together we get the following:

$$F_{PASSIVE-A} = \left((400\ psf)(4.73) + 2(200\ psf)\sqrt{4.73}\right)(5\ ft)(23\ ft)(1.20) = 381\ kips$$

Next, we consider the load contribution on the piles that extend through the crust. From Figure 3.4 and neglecting the small contribution of cohesion in the crust, we get

$$P_{ULT} = (2.86 \cdot 8\ ft + 3.33 \cdot 2\ ft) \cdot 117pcf \cdot 8\ ft$$

$$= 27.6\ {}^{k}/_{ft}$$

Applying equation (2b) and using 0.65 for the GRF (calculated below), we get

$$F_{Piles-A} = 16 \cdot 0.65 \cdot 27.6\ {}^{k}/_{ft} \cdot 4\ ft$$
$$= 1148\ kips$$

Applying equation (8a) we get

$$F_{SIDES-A} = 2 \cdot (400\ psf \cdot Tan(12) + 0.5 \cdot 200\ psf) \cdot 5\ ft \cdot 23\ ft = 43\ kips$$

Summing the loads we get

$$F_{ULT-A} = 381k + 1148k + 43k = 1572\ kips$$

Case B:

From equation (2c) we get:

$$F_{ULT-B} \approx F_{PASSIVE-B} + F_{SIDES-B}$$

Starting with the passive load contribution:

$$F_{PASSIVE-B} = \left(\overline{\sigma_v'}K_p + 2c'\sqrt{K_p}\right)(Z_c - D)(W_T)(k_w)$$

The various terms can be calculated as follows:

$$K_p = Tan^2\left(45 + \frac{34}{2}\right) = 3.54$$

$$K_a = Tan^2\left(45 - \frac{34}{2}\right) = 0.26$$

$$\overline{\sigma_v}' = 5.5\ ft \cdot 117\ {}^{lb}/_{ft^3} = 644\ psf$$

$$k_w = 1 + (3.54 - 0.26)^{\frac{2}{3}}\left(1.1\left(1 - \frac{9}{10}\right)^4 + \frac{1.6}{1 + \frac{5 \cdot 23}{9}} + \frac{0.4(3.54 - 0.26)\left(1 - \frac{9}{10}\right)^3}{1 + \frac{0.05 \cdot 23}{9}}\right) = 1.28$$

Putting this together we get the following:

$$F_{PASSIVE-B} = \left((644\ psf)(3.54) + 2(200\ psf)\sqrt{3.54}\right)(9\ ft)(23\ ft)(1.28) = 803\ kips$$

Applying equation (8a) we get

$$F_{SIDES-B} = 2 \cdot (644\ psf \cdot Tan(12) + 0.5 \cdot 200\ psf) \cdot 9\ ft \cdot 23\ ft = 98\ kips$$

Summing the loads we get

$$F_{ULT-B} = 803k + 98k = 901\ kips$$

Since $F_{ULT-B} < F_{ULT-A}$ Case B controls.

Determination of Δ_{MAX}

From equation (9a) we have

$$\Delta_{MAX} = (T)(0.05 + 0.45\, f_{depth} f_{width})$$

We calculate f_{depth} and f_{width} using equations (9b) and (9c) as follows:

$$f_{depth} = e^{-3\left(\frac{10-1}{9}-1\right)} = 1.0$$

$$f_{width} = \frac{1}{\left(\frac{10}{\frac{23}{9}+4}\right)^4 + 1} = 0.16$$

$$\Delta_{MAX} = (9ft) \cdot \left(12\, {}^{in}/_{ft}\right) \cdot \left(0.05 + 0.45 \cdot (1.0) \cdot (0.16)\right) = 13.2\, in$$

Use 13in

Specification of pile cap p-y curves

The pile cap p-y curve is approximated as shown in Figure 3.1. p_{ULT} is calculated from F_{ULT} as

$$p_{ULT} = \frac{F_{ULT}}{Z_c - D} = \frac{901\, kip}{108\, in} = 8.3\ {}^{k}/_{in}$$

Following Figure 3.1, the user-specified pile cap p-y curves consist of the following points: (0,0), (3.25, 4150), (13, 8300), (100, 8300).

Calculate moment – stiffness behavior of the nonlinear superpile

The development of nonlinear moment-stiffness behavior for input into LPILE 5.0 is described in Section 2.3. We begin by using LPILE 5.0 to calculate the moment-curvature for a single group pile (24-in diameter Cast-In-Steel Shell with 0.5-in shell wall thickness and 7 x #10 bars). The moment is then scaled by the number of group piles (16) while the curvature is unmodified. This curve is then extended to larger ductilities as shown in Figure 2.3.

The case of CISS piles presents an added consideration. The steel shell's contribution to bending stiffness is dependent on its ability to transfer compressive and tensile stresses. Since a CISS pile is typically embedded only 6-inches into the pile cap, these stresses cannot be fully transferred. As there is currently no published guidance on modification to CISS bending stiffness at the pile cap connection, an approximate solution used here is to simply consider only half the steel shell thickness in the bending stiffness computation in the upper diameter of pile length. Both computed stiffness curves are shown in Figure 4.3. A smooth curve fit to the LPILE 5.0 results is also shown. Design moment-stiffness values (based on the smooth curve approximation) are given in Table 4.1. These values are then specified in LPILE 5.0's user-specified moment stiffness option.

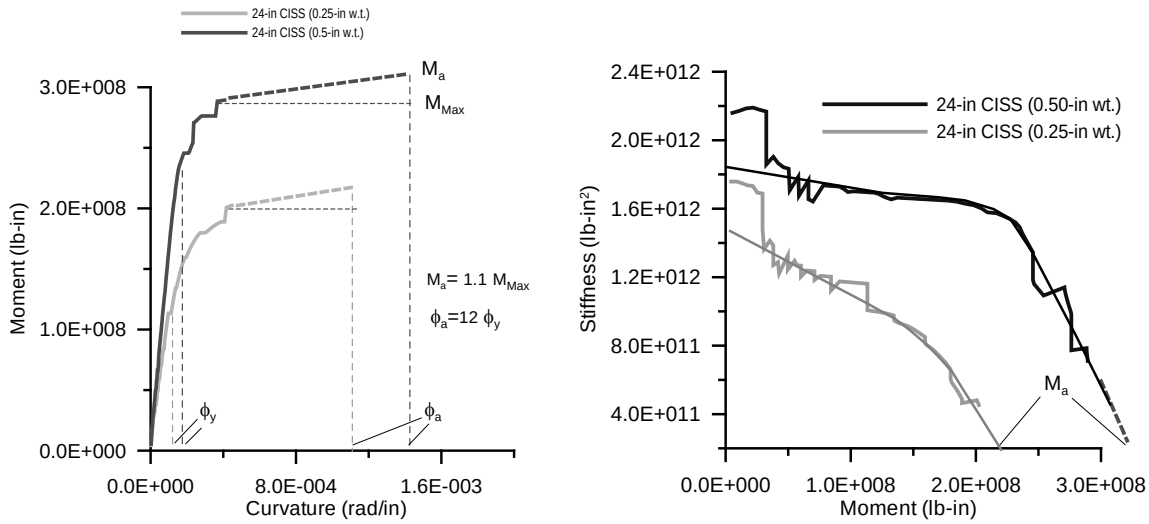

Figure 4.3. Construction of the moment – curvature and moment-stiffness relations for the nonlinear *superpile*

24" CISS (0.25" w.t.)				24" CISS (0.5" w.t.)			
Moment *single pile* (lb-in)	Moment *16 piles* (lb-in)	Stiffness *single pile* (lb-in2)	Stiffness *16 piles* (lb-in2)	Moment *single pile* (lb-in)	Moment *16 piles* (lb-in)	Stiffness *single pile* (lb-in2)	Stiffness *16 piles* (lb-in2)
0.00E+00	0.00E+00	9.39E+10	1.50E+12	0.00E+00	0.00E+00	1.15E+11	1.83E+12
3.92E+06	6.27E+07	7.94E+10	1.27E+12	5.66E+06	9.06E+07	1.08E+11	1.72E+12
7.97E+06	1.27E+08	6.34E+10	1.01E+12	1.25E+07	2.00E+08	1.00E+11	1.61E+12
1.13E+07	1.80E+08	4.33E+10	6.93E+11	1.56E+07	2.49E+08	8.39E+10	1.34E+12
1.24E+07	1.99E+08	3.06E+10	4.89E+11	1.67E+07	2.68E+08	6.54E+10	1.05E+12
1.39E+07	2.22E+08	1.28E+10	2.05E+11	1.82E+07	2.91E+08	4.22E+10	6.76E+11
				1.99E+07	3.19E+08	1.37E+10	2.19E+11

Table 4.1. Moment-stiffness values for a nonlinear single pile and 16 pile *superpile* (based on smooth curves shown in Figure 4.3).

Rotational stiffness

Rotational stiffness is estimated following Section 3.3. Assuming a design capacity of 200 kips, the axial stiffness of a single pile is estimated as

$$K_{ax} = \frac{(0.75)(2)(200k)}{0.25\ in} = 1200k/in$$

The rotational stiffness for the pile group is then estimated as

$$K_\theta = \left(144\,\frac{in^2}{ft^2}\right)(4(-9ft)^2 + 4(-3ft)^2) + 4(3ft)^2) + 4(9ft)^2\left(1200\,{}^{k}/_{in}\right) = 1.2 \times 10^8 k - in$$

This value is specified as a rotational restraint at the top of the super pile.

p-y scaling and Group Reduction Factors

From Figure 3.6, 3 diameter pile spacing corresponds to a leading row reduction factor of 0.82, a second row reduction factor of 0.67, a third row factor of 0.58, and a trailing row reduction factor of 0.52. Using an average GRF of 0.65, we scale by 16 to account for the number of piles. Thus, for nonliquefiable soils, the GRF = (0.65)(16) = 10.4

For the liquefiable layer, two options are available. In the analysis that follows the Residual Strength Option was used. For clarity, p-multiplier results are given as well.

<u>p-multiplier option</u>

If this option is selected the p-multiplier is calculated using the relation in Figure 3.7:

$$m_p = 0.0031 \cdot N + 0.00034 \cdot N^2 = 0.14 \qquad \text{(upper zone)}$$

$$= 0.065 \qquad \text{(lower zone)}$$

Thus,

$$GRF_{liq} = (16) \cdot (0.14) = 2.2 \qquad \text{(upper zone)}$$

$$= (16) \cdot (0.065) = 1.0 \qquad \text{(lower zone)}$$

<u>Residual strength option</u>

Using the residual strength method the p-y curves for liquefied soil are constructed based on the Matlock (1974) soft clay p-y model using the residual strength of the liquefied layer as the undrained strength of the soft clay. Residual strengths were calculated in Step 2 as 425 psf for the upper loose sand zone and 255 psf for the lower zone.

In liquefiable zones a GRF of 16 is applied, corresponding to the number of piles in the pile group. Regardless of the modeling option chosen (p-multiplier or residual strength) the GRF does not include a group efficiency adjustment in the liquefied region.

Softening near the liquefaction interface

From Figure 3.8, we get

$$S_b = 2 - \frac{(2-1)}{2} = 1.5$$

Thus, at the lower liquefaction boundary, p_{ult} is assumed to vary linearly from the liquefied resistance to the full resistance of the neighboring layer over a length of 1.5 pile diameters, or 3 feet. No adjustment is required at the upper liquefaction boundary since Case B controls and the soil above the boundary is treated as a composite cap-pile-soil block. Adjustments to the GRF below the lower liquefaction boundary can be made in 3 increments according to Table 4.2. Note that P_L/P_H is approximately equal to m_p.

Distance from interface (ft)	GRF Adjustment Factor	GRF Adjustment Bottom Interface
1	$\frac{1}{3}+\frac{2P_L}{3P_H}$	.38
2	$\frac{2}{3}+\frac{P_L}{3P_H}$	.69
3	1	1

Table 4.2: Adjustment to the GRF of stiff soil near the liquefaction interface. P_L and P_H correspond to the P_{ult} of the liquefied layer and the nonliquefied layer, respectively.

Summary of Group Reduction Factors (or p-y adjustment factors)

Table 4.3 gives a summary of the recommended GRF's for the LPILE 5.0 model:

Depth from top of cap (ft)	GRF
0 - 9	1
9 - 19	16
19 - 20	4.0
20 - 21	7.2
21 - 40	10.4

Table 4.3. Group Reduction Factor (GRF) summary

Impose soil displacement and inertial loads on the foundation

The 39-in crust displacement calculated in Step3 is imposed on the *superpile* along with inertial shear loads from the superstructure and pilecap. Given the high levels of shaking in this example, it is assumed that the column will develop a plastic hinge. As given in Figure 3.10, this hinge limits the shear force from the superstructure to

$$V_{SHEAR} = \frac{M_o}{H} = \frac{12{,}000\ kip - ft}{20\ ft} = 600 kips$$

An additional shear force due to the inertial loading of the pile cap must also be considered. From equation (15) we get:

$$V_{CAP} = (5\ ft)(23\ ft)(23\ ft)\left(0.15\frac{kips}{ft^3}\right)(0.5)(0.65) = 129\ kips$$

From equation (13a) or (13b), 50% of the total inertial shear force is combined with the kinematic loading. Thus,

$$V_i = (0.5)(600 kips + 129\ kips) = 365\ kips$$

Step 5: Evaluate results against foundation performance criteria

The results from the LPILE 5.0 foundation analysis with a 39-inch imposed soil displacement and 365 kip shear load applied at the top of the pile cap is presented in Figure 4.4. The analysis predicts a pile cap displacement of 5.3-inches, which satisfies the H/20 displacement criteria of Table 3.1. A summary of the peak moment demands is given in Table 4.4.

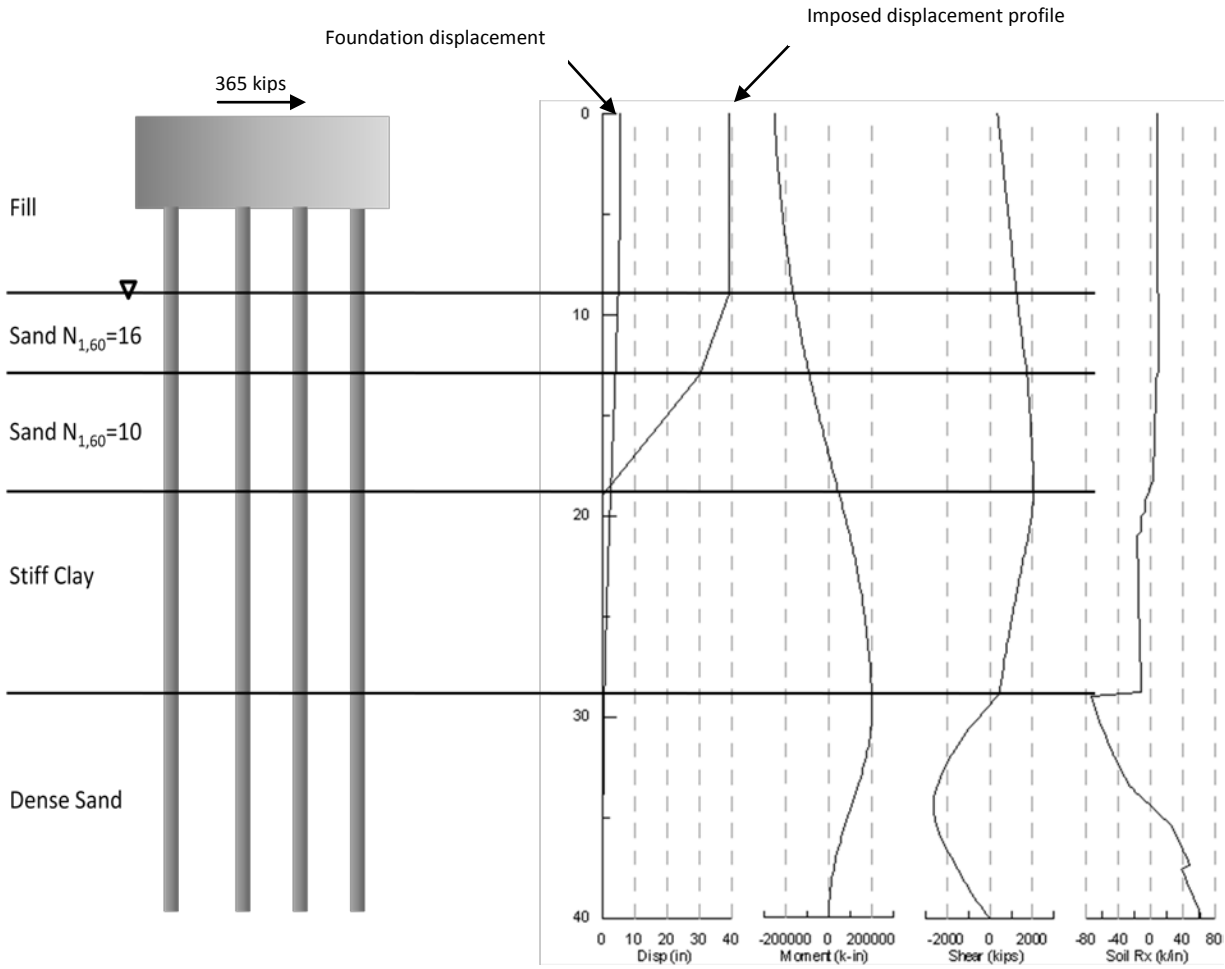

Figure 4.4. Profiles of displacement, moment, shear, and soil reaction resulting from an imposed displacement profile with maximum displacement of 39 inches.

Pile Section	Kinematic + Inertia M_{max} (kip-in)	Kinematic – Inertia M_{max} (kip-in)	Allowable Moment (kip-in)
0 to 2 ft	215,000	124,000	222,000
> 2 ft	204,000	102,000	319,000

Table 4.4. Maximum moment demand and allowable moments

Adequacy of pile shear capacity is typically performed by Office of Structural Design and follows SDC Section 3.6. It is rare for a pile to have sufficient moment capacity while not having adequate shear capacity. Only moment capacity is checked in this example.

4.2 Foundation Restrained Soil Displacement Example

Problem description

The example concerns the evaluation of the abutment shown in Figure 4.5. The abutment is underlain by soft clay, loose sand, and then dense sand. Assumed material properties and layer thicknesses are given in the figure. The abutment configuration and pile layout are shown in Figure 4.6.

Loading consists of a combined design dead load and live load of 200 kips/pile. The 5% in 50 year seismic load is 0.5g peak ground acceleration (PGA) corresponding to a magnitude 7.5 event.

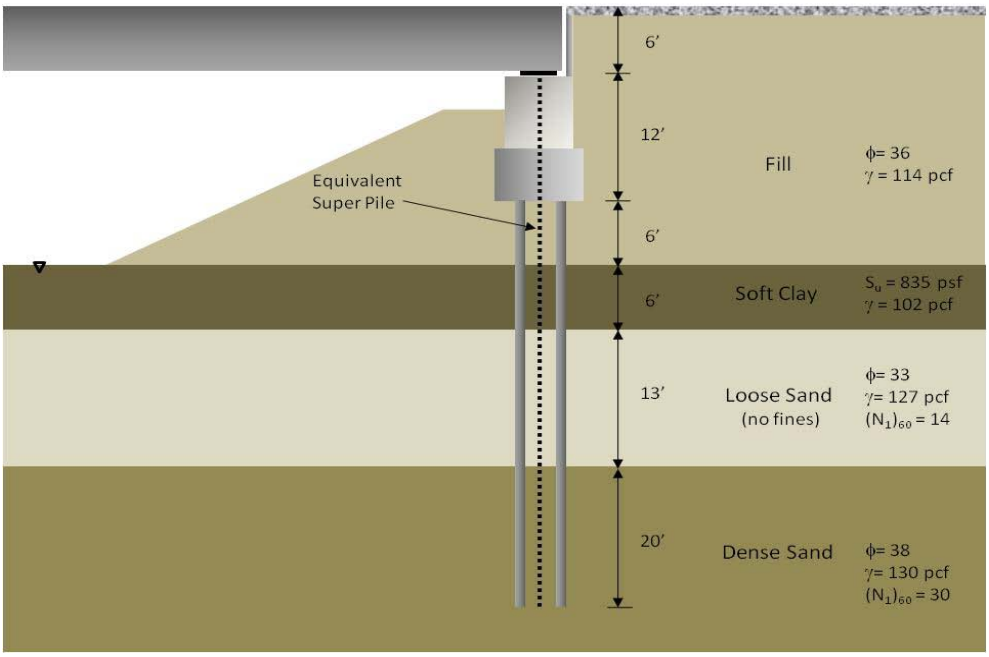

Figure 4.5. Abutment configuration and soil properties

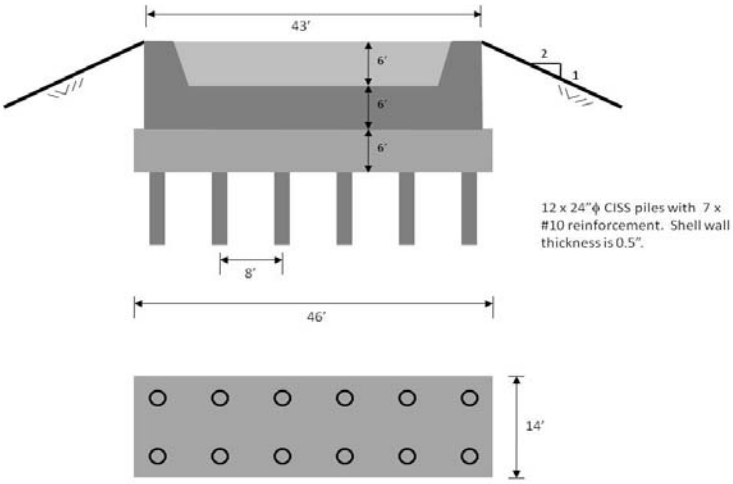

Figure 4.6. Abutment section and pile layout

Problem solution

Since the abutment has a limited footprint, the abutment foundation can act to restrain the soil displacement demand stemming from the embankment. Thus, we follow the procedures outlined in Section 3.7 for the Foundation Restrained Displacement design case.

Step 1: Assess liquefaction potential of each layer.

The depth to the center of the loose sand layer varies from 12.5 feet to 36.5 feet, depending whether it is measured from the base of the embankment or the top of the embankment. For the assessment of liquefaction potential, an average depth of 24.5 feet is used. Following Youd (2001), the cyclic resistance ratio, CRR, is calculated as

$$CRR = CRR_{\sigma_v'=1,\alpha=0} \cdot K_\sigma \cdot K_\alpha$$

where $CRR_{\sigma_v'=1,\alpha=0}$ is estimated to be 0.16g (for the case of $(N_1)_{60CS} = 14$), $K_\sigma \sim 1$, and $K_\alpha \sim 1.2$. Thus CRR ~ 0.19.

The cyclic stress ratio, CSR, can be estimated as

$$CSR = 0.65\,\frac{\sigma_v}{\sigma_v{}'}\frac{A_{max}}{g}r_d = 0.65\,\frac{2806\,psf}{2026\,psf}\cdot 0.5 \cdot 0.9 = 0.41$$

Thus the factor of safety against liquefaction triggering is

$$FS_{liq} = \frac{CRR}{CSR} = \frac{0.19}{0.41} = 0.46$$

Since FS_{liq} <1, the loose sand layer is very susceptible to liquefaction for the design loading.

A similar analysis is performed for the top of the dense sand layer. In this case

$$CRR = 0.48 \cdot 1 \cdot 1.2 = 0.58$$

$$CSR = 0.65 \cdot \frac{3632psf}{2446psf} \cdot 0.5 \cdot 0.9 = 0.43$$

$$FS_{liq} = \frac{CRR}{CSR} = \frac{0.58}{0.43} = 1.35$$

Since FS_{liq} is much larger than 1, it can be assumed that the dense sand layer will not liquefy.

Step2: Determine residual strengths for the center of the loose sand layer. Since equation (11) is functionally dependent on effective overburden stress, the residual strength is calculated in three zones: the bottom of the embankment, midslope, and at the top of the embankment. The results are given in Table 4.5.

Embankment zone	σ_v' (psf)	S_r(psf)
bottom	658	251
midslope	2026	444
top	3394	589

Table 4.5. Residual strengths by location

Step 3: Develop foundation model.

p-y curves for the pile cap

Per Section 3.1, the ultimate crust load, F_{ULT}, must be evaluated for the two design cases shown in Figure 3.3.

Case A:

From equation (2a) we get:

$$F_{ULT-A} \approx F_{PASSIVE-A} + F_{PILES-A} + F_{SIDES-A}$$

From Section 3.1, equation (3) we get

$$F_{PASSIVE} = \overline{\sigma_v}' \cdot K_p \cdot T \cdot W_T \cdot k_w$$

Calculating the terms of the right hand side of the equation, we get the following:

$$\overline{\sigma_v}' = 12\ ft\ \cdot 114\ {}^{lb}/_{ft^3} = 1368\ psf$$

$$K_p = Tan^2\left(45 + \tfrac{36}{2}\right)\left(1 + (0.8152 - 0.0545\ \cdot 36 + 0.001771\ \cdot 36^2)\frac{12}{36} - 0.15\left(\frac{12}{36}\right)^2\right) = 5.26$$

δ was assumed to be 1/3 of ϕ.

$$K_a = Tan^2\left(45 - \frac{36}{2}\right) = 0.26$$

$$k_w = 1 + (5.26 - 0.26)^{\frac{2}{3}}\left(1.1\left(1 - \frac{12}{18}\right)^4 + \frac{1.6}{1 + \frac{5 \cdot 44}{12}} + \frac{0.4(5.26 - 0.26)\left(1 - \frac{12}{18}\right)^3}{1 + \frac{0.05 \cdot 44}{12}}\right) = 1.46$$

The development of k_w by Ovesen(1964) assumes a flat ground surface. Because the resisting soil mass is an embankment of finite width (sloping to the sides at 2:1) the full 3D soil wedge cannot be developed. Since there are no procedures available to correct for the finite width of the resisting mass, a 20% reduction to the wedge effect is applied based on engineering judgment. Thus

$$k_w = 1 + 0.8 \cdot 0.46 = 1.37$$

Putting this together, we get

$$F_{PASSIVE-A} = (1368psf) \cdot (5.26) \cdot (12ft) \cdot (44ft) \cdot (1.37) = 5205\ kips$$

Next, we consider the load contribution on the piles that extend through the crust. From Figure 3.4 we get

$$P_{ULT-SAND} = (3.41 \cdot 21\ ft + 3.68 \cdot 2\ ft) \cdot 114pcf \cdot 21\ ft$$
$$= 189\ {}^{k}/_{ft}$$

$$P_{ULT-CLAY} = 9 \cdot 835\ psf \cdot 2\ ft$$
$$= 15\ {}^{k}/_{ft}$$

Applying equation (2b) and using 0.83 for the GRF (calculated below), we get

$$F_{Piles-A} = \left(189\ {}^{k}/_{ft} \cdot 6\,ft + 15\ {}^{k}/_{ft} \cdot 6\,ft\right)\ 0.83 \cdot 12\,piles$$
$$= 12191\,kips$$

Applying equation (8a) we get

$$F_{SIDES-A} = 2 \cdot \left(1368\,psf \cdot Tan(12)\right) \cdot 12\,ft \cdot 14\,ft = 98\,kips$$

Summing the loads we get

$$F_{ULT-A} = 5205k + 12191k + 98k = 17494\,kips$$

Case B:

From equation (2c) we get:

$$F_{ULT-B} \approx F_{PASSIVE-B} + F_{SIDES-B}$$

Starting with the passive load contribution:

$$F_{PASSIVE-B} = \left(\overline{\sigma_v'}K_p + 2c'\sqrt{K_p}\right)(Z_c - D)(W_T)(k_w)$$

The various terms can be calculated as follows:

$$K_p = Tan^2\left(45 + \tfrac{36}{2}\right) = 3.85$$

$$K_a = Tan^2\left(45 - \frac{36}{2}\right) = 0.26$$

$$\overline{\sigma_v}' = {}^{(6+24)}/_{2}\ ft \cdot 114\ {}^{lb}/_{ft^3} = 1710\,psf$$

$$k_w = 1 + (3.85 - 0.26)^{\frac{2}{3}}\left(1.1\left(1 - \frac{24}{30}\right)^4 + \frac{1.6}{1 + \frac{5 \cdot 44}{24}} + \frac{0.4(3.85 - 0.26)\left(1 - \frac{24}{30}\right)^3}{1 + \frac{0.05 \cdot 44}{24}}\right) = 1.40$$

As in Case A, we correct for the finite width of the resisting mass by taking a 20% reduction to the wedge effect. Thus

$$k_w = 1 + 0.8 \cdot 0.40 = 1.32$$

Putting this together we get the following:

$$F_{PASSIVE-B} = \left((1710\,psf)(3.85)(18\,ft) + 2(835\,psf)\left(\sqrt{3.85}\right)(6\,ft)\right)(44\,ft)(1.32)$$
$$= 8025\,kips$$

Applying equation (8a) we get

$$F_{SIDES-B} = 2 \cdot (18\,ft \cdot 1710\,psf \cdot Tan(12) + 0.5 \cdot 835\,psf \cdot 6\,ft) \cdot 14\,ft$$

$$= 253\,kips$$

Summing the loads we get

$$F_{ULT-B} = 8025k + 253k = 8278\,kips$$

Since $F_{ULT-B} < F_{ULT-A}$ Case B controls.

Determination of Δ_{MAX}

From equation (9a) we have

$$\Delta_{MAX} = (T)(0.05 + 0.45\,f_{depth} f_{width})$$

We calculate f_{depth} and f_{width} using equations (9b) and (9c) as follows:

$$f_{depth} = e^{-3(\frac{30-6}{24}-1)} = 1$$

$$f_{width} = \frac{1}{\left(\frac{10}{\frac{44}{24}+4}\right)^4 + 1} = 0.10$$

$$\Delta_{MAX} = (24ft) \cdot \left(12\,{}^{in}/_{ft}\right) \cdot \left(0.05 + 0.45 \cdot (1.0) \cdot (0.10)\right) = 27\,in$$

Specification of pile cap p-y curves

The pile cap p-y curve is approximated as shown in Figure 3.1. p_{ULT} is calculated from F_{ULT} as

$$p_{ULT} = \frac{F_{ULT}}{T} = \frac{8278\,kip}{288\,in} = 28.7\,{}^{k}/_{in}$$

Following Figure 3.1, the user-specified pile cap p-y curves consist of the following points: (0,0), (6.75, 14370), (27, 28700), (100, 28700).

Modeling the piles

Use LPILE 5.0 to calculate the moment-curvature for a single group pile (24-in diameter Cast-In-Steel Shell with 0.5-in shell wall thickness and 7 x #10 bars). Scale the moment by the number of group piles (12). Follow the moment-curvature construction described in Section 2.3.

Similar to Example Problem 4.1, the stiffness of the upper portion of the CISS pile is modified to account for the pile's inability fully transfer compressive and tensile stresses in bending since the pile's steel shell is typically developed only 6 inches into the pile cap. As there is currently no published guidance on modification to bending stiffness at pile cap connections, an approximate solution used here is to simply consider only half the steel shell thickness in the bending stiffness computation in the upper diameter of pile length. Both computed stiffness curves are shown in Figure 4.7. A smooth curve fit to the LPILE 5.0 results is also shown. Recommended moment-stiffness values (based on the smooth curve approximation) are given in Table 4.6.

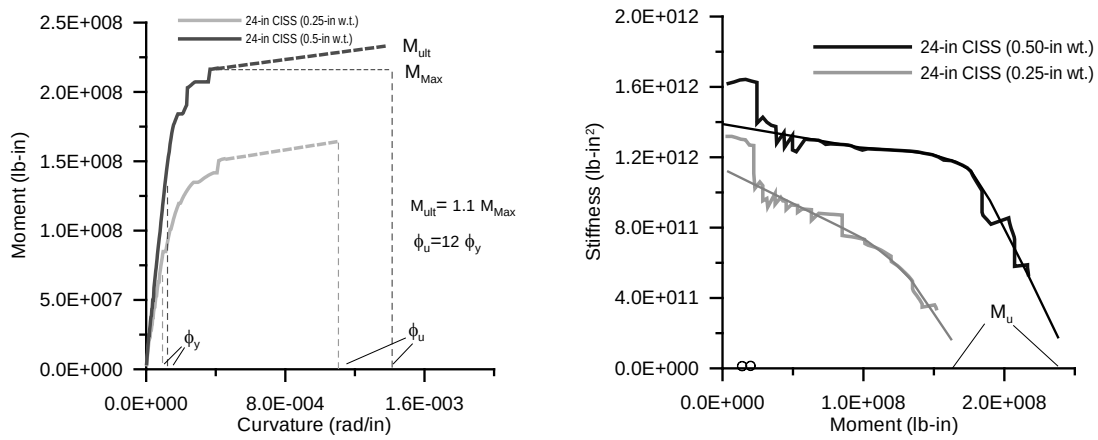

Figure 4.7. Moment-curvature and moment-stiffness curves calculated using LPILE-5. A design axial load of 200k was used. For beam-column models that do not incorporate a confined concrete strength (such as LPILE-5), the moment-curvature curve is extrapolated by assuming an additional 10% moment capacity is developed at a curvature ductility of 12.

24" CISS (0.25" w.t.)				24" CISS (0.5" w.t.)			
Moment *single pile* (lb-in)	Moment *12 piles* (lb-in)	Stiffness *single pile* (lb-in2)	Stiffness *12 piles* (lb-in2)	Moment *single pile* (lb-in)	Moment *12 piles* (lb-in)	Stiffness *single pile* (lb-in2)	Stiffness *12 piles* (lb-in2)
0.00E+00	0.00E+00	9.39E+10	1.13E+12	0.00E+00	0.00E+00	1.15E+11	1.37E+12
3.92E+06	4.70E+07	7.94E+10	9.52E+11	5.66E+06	6.79E+07	1.08E+11	1.29E+12
7.97E+06	9.56E+07	6.34E+10	7.60E+11	1.25E+07	1.50E+08	1.00E+11	1.20E+12
1.13E+07	1.35E+08	4.33E+10	5.20E+11	1.56E+07	1.87E+08	8.39E+10	1.01E+12
1.24E+07	1.49E+08	3.06E+10	3.67E+11	1.67E+07	2.01E+08	6.54E+10	7.85E+11
1.39E+07	1.67E+08	1.28E+10	1.54E+11	1.82E+07	2.18E+08	4.22E+10	5.07E+11
				1.99E+07	2.39E+08	1.37E+10	1.64E+11

*CISS includes 7 x #10 longitudinal bars

Table 4.6. Moment-stiffness values for a nonlinear single pile and 12 pile *superpile* (based on smooth curves shown in Figure 4.6).

Rotational stiffness

Rotational stiffness is estimated following Section 3.3. Assuming a design capacity of 200 kips, the axial stiffness of a single pile is estimated as

$$K_{ax} = \frac{(0.75)(2)(200k)}{0.25\ in} = 1200k/in$$

The rotational stiffness for the pile group is then estimated as

$$K_\theta = \left(144\,\frac{in^2}{ft^2}\right)(6(-5ft)^2 + 6(5ft)^2)\left(1200\,{}^{k}/_{in}\right) = 5.2 \times 10^7 k - in$$

This value is specified as a rotational restraint at the top of the super pile.

p-y scaling and Group Reduction Factors

From Figure 3.6, 4 diameter pile spacing corresponds to a leading row reduction factor of 0.88 and a trailing row reduction factor of 0.78. Using an average GRF of 0.83, we scale by 12 to account for the number of piles. Thus, for nonliquefiable soils, the GRF = (0.83)(12) = 10.

For the liquefiable layer, two options are available. In the analysis that follows the Residual Strength Option was used. For clarity, p-multiplier results are given as well.

<u>p-multiplier option</u>

If this option is selected the p-multiplier is calculated using the relation in Figure 3.7:

$m_p = 0.0031 \cdot N + 0.00034 \cdot N^2$=$0.0031 \cdot 14 + 0.00034 \cdot 14^2 = 0.11$

Thus,

$$GRF_{liq} = (12) \cdot (0.11) = 1.32$$

<u>Residual strength option</u>

Using the residual strength method the p-y curves for liquefied soil are constructed based on the Matlock (1974) soft clay p-y model using the residual strength of the liquefied layer as the undrained strength of the soft clay. For p-y modeling, the residual strength is taken from Table 4.5 for the top of slope location (589 psf).

In both regions a GRF of 12 is applied, corresponding to the number of piles in the pile group. Regardless of the modeling option chosen (p-multiplier or residual strength) the GRF does not include a group efficiency adjustment in the liquefied region.

Softening near the liquefaction interface

From Figure 3.8, we get

$$S_b = 2 - \frac{(2-1)}{2} = 1.5$$

Thus, at the lower liquefaction boundary, p_{ult} is assumed to vary linearly from the liquefied resistance to the full resistance of the neighboring layer over a length of 1.5 pile diameters, or 3 feet. No adjustment is required at the upper liquefaction boundary since Case B controls and the soil above the boundary is treated as a composite cap-pile-soil block. Adjustments to the GRF below the lower liquefaction boundary can be made in 3 increments according to Table 4.7. Note that ${}^{P_L}/_{P_H}$ is approximately equal to m_p.

Distance from interface (ft)	GRF Adjustment Factor	GRF Adjustment Bottom Interface
1	$\frac{1}{3}+\frac{2P_L}{3P_H}$	.41
2	$\frac{2}{3}+\frac{P_L}{3P_H}$	.70
3	1	1

Table 4.7: Adjustment to the GRF of stiff soil near the liquefaction interface. P_L and P_H correspond to the P_{ult} of the liquefied layer and the nonliquefied layer, respectively.

Summary of Group Reduction Factors (or p-y adjustment factors)

A summary of the recommended GRF's for the LPILE 5.0 model is given in Table 4.8:

Depth Interval (ft)	GRF
0 - 24	1
24 - 37	12
37 - 38	4.1
38 - 39	7
39 - 57	10

Table 4.8. Group Reduction Factor (GRF) summary

Step 4: Impose a series of increasing displacement profiles on the *superpile* as depicted in Figure 2.2. For each displacement profile, the *superpile* shear force at the midpoint of the liquefied layer is tabulated as shown in Table 4.9.

Imposed soil disp (in)	Pile cap disp (in)	Shear at liq. zone midpoint (kips)	Running average shear (kips)
0	0	0	0
1	0.9	322	161
2	1.7	582	301
3	2.6	780	421
4	3.4	1010	539
6	5.1	1330	671
8	7.1	1560	798
10	9.1	1670	907

Table 4.9. LPILE 5.0 pushover results.

Step 5: Calculate F_{DECK}

In this example problem we assume that the interior bridge bents and opposite abutment are stiff enough to resist the sliding of the abutment mass through load transfer through the bridge deck. This resistance force is limited by the ultimate passive resistance of the soil behind the abutment back wall. This force is calculated using equation (3), with K_p *(log-spiral)* = 5.26, c = 0, and an assumed deck thickness of 6 feet. Thus,

$$F_{DECK} = \left(\overline{\sigma_v'}K_p + 2c\sqrt{K_p}\right)(T_{DECK})W_T = (3ft)\cdot(114pcf)\cdot(5.26)\cdot(6ft)\cdot(43ft) = 464\ kips$$

Steps 6and 7: Perform slope stability analyses of the embankment to determine the yield coefficient (k_y) for a range of resisting forces.

The embankment profile is modeled in a slope stability program (see Figure 4.8). Since the residual strength of the liquefiable layer is dependent on overburden stress, several strength zones are defined in the model, following Table 4.5. Potential failure surfaces are block type and constrained to pass through the midpoint of the liquefiable layer. Two resistive point loads are applied to the slope. The first load corresponds to F_{DECK}. Since the slope stability analyses are performed on a unit width basis, F_{DECK} must be divided by the abutment width before being applied as a point load. Following Figure 3.15, the effective abutment width is 68 feet. Thus, the deck point load is calculated as

$$F_{DECK1} = \frac{464\ kips}{68\ ft} = 6.8\ {}^{k}/_{ft}$$

The second point load ***R*** is due to the shear resistance developed by the abutment foundation. A range of ***R*** values are considered in the analysis.

The yield coefficient k_y is determined by specifying a foundation resistance force ***R*** and determining the seismic load coefficient that results in a factor of safety (FS) equal to 1. This analysis is repeated for a range of ***R***. Alternatively, k_y can be specified initially and the slope stability analysis can be performed to determine the ***R*** that results in a FS of 1.0. Table 4.10 shows the results from these analyses.

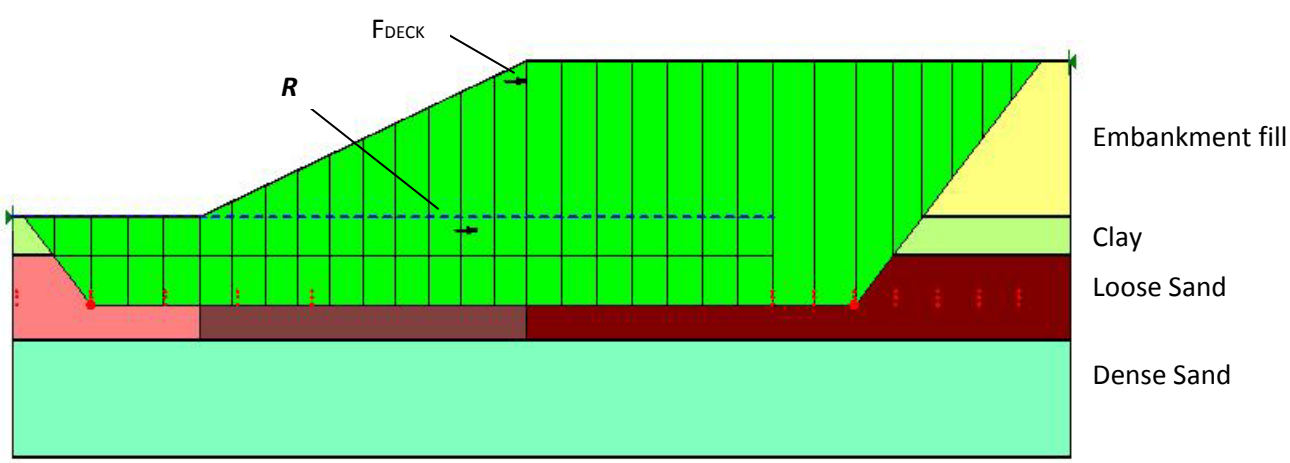

Figure 4.8. Slope stability model used to relate the foundation resistance force ***R*** to the seismic coefficient k_y

K_y	R (kips/ft)	R x W_T (kips)	D (in)
0.14	0	0	5.3
0.15	8	544	4.7
0.16	15	1020	4.1
0.18	27	1836	3.2
0.20	40	2720	2.6
0.22	52	3536	2.1

Table 4.10. Slope stability results (K_y as a function of R). Displacements determined using Bray and Travasarou, 2007

Step 8: Calculate the slope displacement corresponding to k_y.

Equation (16) is used to calculate the slope displacement corresponding to the k_y values in Table 4.10. The results are given in the fourth column of Table 4.10.

Step 9: Plot the displacement compatibility curve

Data from Tables 4.9 and 4.10 are plotted to determine the points of displacement compatibility. As discussed in Section 3.7, the running average shear (fourth column in Table 4.9) must be used to capture the average foundation load-resistance behavior. Also, since R in Table 4.10 was calculated on a per unit width base, R must be multiplied by the tributary width of the foundation (see Figure 3.15) to compare to the running average shears of Table 4.9. The resulting plot is given in Figure 4.9.

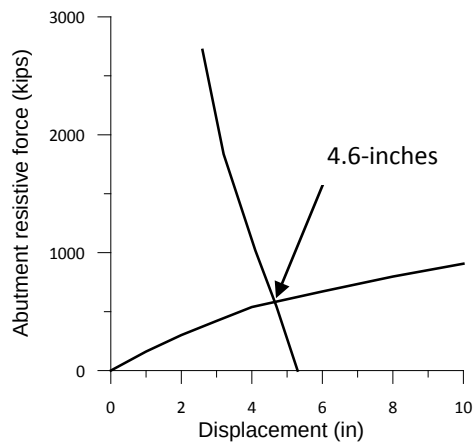

Figure 4.9. Displacement compatibility plot

Step 10: Evaluate results against foundation performance criteria

In order to calculate foundation demands, 4.6 inches of soil displacement is imposed on the LPILE 5.0 foundation model. Figure 4.10 presents the displacement, moment, shear, and soil reaction resulting from the imposed displacement profile. The resulting pile cap displacement is 3.9 inches, which satisfies the D < 12-inch criteria of Table 3.1. Maximum moment demand at the top of pile (which was modeled as having a reduced section) and within the remaining pile section are given in Table 4.11.

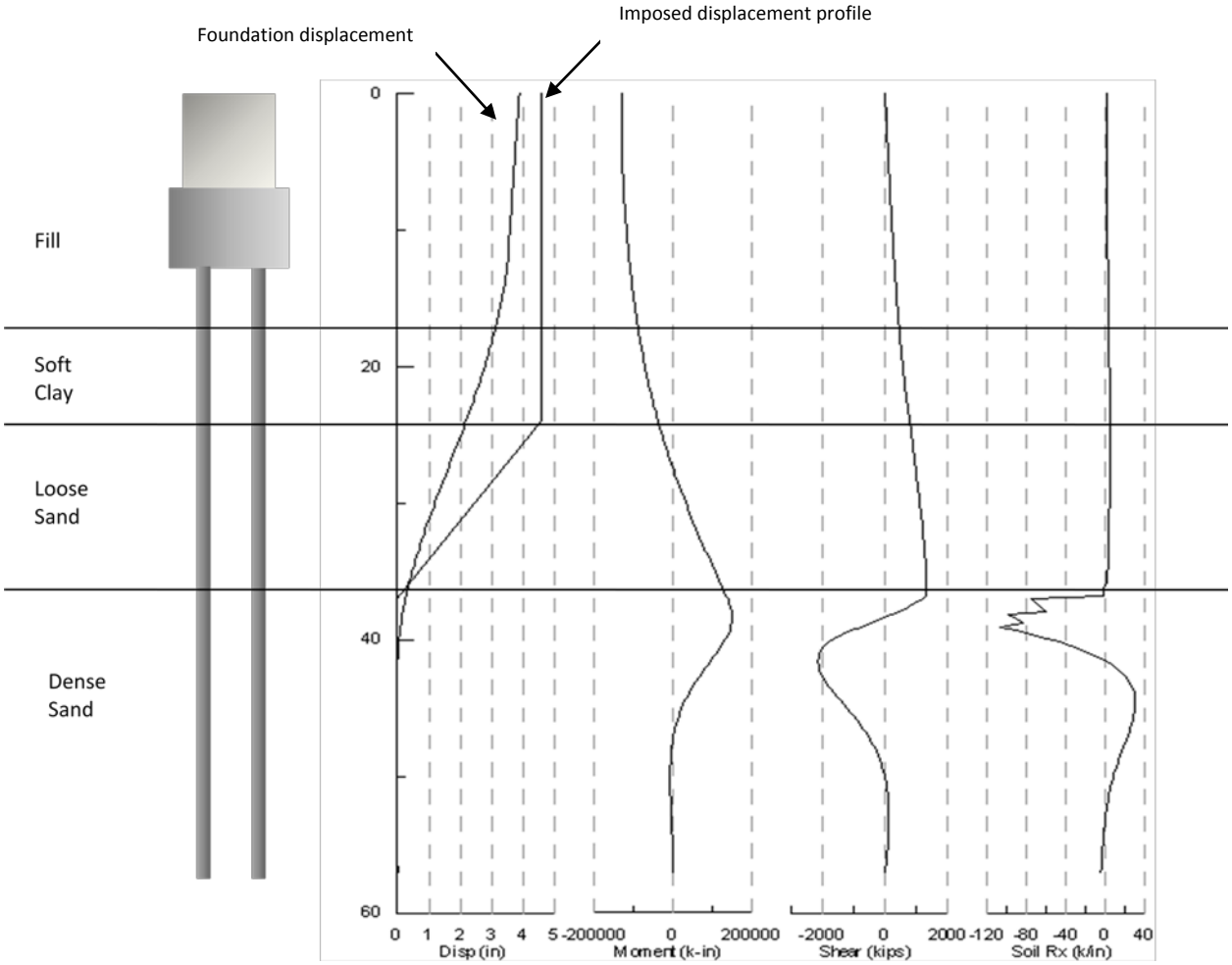

Figure 4.10. Profiles of displacement, moment, shear, and soil reaction resulting from an imposed displacement profile with maximum displacement of 4.6 inches.

Pile Section	Max Moment Demand (kip-in)	Allowable Moment (kip-in)
0 to 2 ft	83,900	167,000
> 2 ft	151,000	239,000

Table 4.11. Maximum moment demand and allowable moments

Adequacy of pile shear capacity is typically performed by Office of Structural Design and follows SDC Section 3.6. It is very rare for a pile to have sufficient moment capacity while not having adequate shear capacity. Only moment capacity is checked in this example.

References

American Petroleum Institute (API), "Recommended Practice for Planning, Designing and Constructing Fixed Offshore Platforms – Working Stress Design", RP 2A-WSD, 20th Edition, July 1, 1993, American Petroleum Institute, Washington, DC

Ashford, S., Boulanger, R., and Brandenberg, S. (2010) "Recommended Design Practice for Pile Foundations in Laterally Spreading Ground." Report PEER 2010/XX, Pacific Earthquake Engineering Research Center (PEER), Berkeley, CA

ATC/MCEER, 2002, *Comprehensive Specification for the Seismic Design of Bridges*, NCHRP Report 472, National Cooperative Research Program, Washington, DC.

Brandenberg, S.J., Boulanger, R.W., Kutter, B.L., and Chang, D. (2007). "Liquefaction-induced softening of load transfer between pile groups and laterally spreading crusts." *J. Geotech. Geoenviron. Eng*., ASCE, 133(1), 91-103

Bray, J.D., and Travasarou, T. (2007). "Simplified procedure for estimating earthquake-induced deviatoric slope displacements." *J. Geotech. Geoenviron. Eng.*, 133(4): 381-392.

Cetin, K.O., Seed, R.B., Der Kiuregian, A., Tokimatsu, K., Harder, L.F., Kayen, R.E., and Moss, R.E.S. (2004). "Standard penetration test-based probabilistic and deterministic assessment of seismic soil liquefaction potential." *J. Geotech. Geoenviron. Eng.*, 130(12): 1314-1340.

Faris, A.T., 2004. *Probabilistic Models for Engineering Assessment of Liquefaction-Induced Lateral Spreading Displacements*, Ph.D. thesis, University of California at Berkeley, 436 pp.

Faris, A.T., Seed, R.B., Kayen, R.E., and Wu, J., 2006. A semi-empirical model for the estimation of maximum horizontal displacement due to liquefaction-induced lateral spreading, *8th National Conference on Earthquake Engineering*, EERI, San Francisco, CA

Idriss, I.M., and Boulanger, R.W., 2008, *Soil Liquefaction During Earthquakes*, Earthquake Engineering Research Institute, Oakland, CA, 235 pp.

Kramer, S.L., Wang, C.H. (2010) *publication pending*

Matlock, H. (1970). "Correlations of design of laterally loaded piles in soft clay." *Proc. Offshore Technology Conference*, Houston, TX, Vol. 1, No. 1204, pp. 577-594.

Mokwa, R.L., and Duncan, J.M. (2000). "Experimental evaluation of lateral-load resistance of pile caps." *J. Geotech. Geoenviron. Eng.*, ASCE. 127(2). 185-192.

Mokwa, R.L., and Duncan, J.M., "Investigation of the Resistance of Pile Caps and Integral Abutments to Lateral Loading", Final Contract Report, February 2000, Virginia Transportation Research Council, Charlottesville, VA

Ovesen, N. K. (1964). *Anchor slabs, calculation methods and model tests*. Bulletin No. 16, The Danish Geotechnical Institute, Copenhagen.

Reese, L.C., W.R. Cox, and F.D. Koop, "Analysis of Laterally Loaded Piles in Sand", Paper No. OTC 2080, Proceedings, Fifth Annual Offshore Technology Conference, Houston, Texas, 1974 (GESA Report No. D-75-9).

Reese, L.C. and R.C. Welch, "Lateral Loading of Deep Foundations in Stiff Clay", Journal of the Geotechnical Engineering Division, American Society of Civil Engineers, Vol. 101, No. GT7, Proceedings Paper 11456, 1975, pp. 633-649 (GESA Report No. D-74-10).

Reese, L. C., Wang, S. T., Isenhower, W. M., Arrelaga, J.A., and Hendrix, J. A., 2005. "LPILE Plus Version 5.0," Ensoft, Inc. Austin, TX.

Seed, R.B., Cetin, K.O., Moss, R.E.S., Kammerer, A., Wu, J., Pestana, J., Riemer, M., Sancio, R.B., Bray, J.D., Kayen, R.E., and Faris, A., 2003. *Recent Advances in Soil Liquefaction Engineering: a Unified and Consistent Framework*, Keynote presentation, 26th Annual ASCE Los Angeles Geotechnical Spring Seminar, Long Beach, CA.

Youd, T.L., Idriss, I.M. Andrus, R.D. Arango, I., Castro, G., Christian, J.T., Dobry, R., Liam Finn, W.D.L., Harder, L.F., Jr., Hynes, M.E., Ishihara, K., Koester, J.P., Liao, S.S.C., Marcuson, W.F., III, Martin, G.R., Mitchell, J.K., Moriwaki, Y., Power, M.S., Robertson, P.K., Seed, R.B., Stokoe, K.H., II, (2001). "Liquefaction Resistance of Soils: Summary Report from the 1996 NCEER and 1998 NCEER/NSF Workshops on Evaluation of Liquefaction Resistance of Soils", *J. of Geotech. Geoenviron. Eng.* 127(10) 817-833 (republication 137 with correct authors).

Zhang, G., Robertson, P.K., and Brachman, R.W.I. (2004). "Estimating liquefaction-induced lateral displacements using the standard penetration test or cone penetration test." *J. Geotech. Geoenviron. Eng.*, 130(8): 861-871.

Errata: (1/31/12) Equation (7) was corrected by removing an extra (D + T)

Appendix A: Numerical Estimation of γ_{max}

The following routine provides a numerical approximation for the Strain Potential Index (γ_{max}) as shown in Figure 3.11. This routine incorporates an estimate of limiting shear strain by Idriss and Boulanger (2008) that is then modified to account for dependence on cyclic stress ratio (CSR) following the general curve shapes of Wu (2002). Lines l_1 and l_2 are introduced to define γ_{max} at low values of CSR. Despite the cobbled together nature of the routine, it provides a reasonably accurate approximation of Figure 3.11 while being simple enough to implement in a spreadsheet.

$$\gamma_{max} = \begin{cases} 0 & CSR \leq 0.04 \\ \left(\frac{CSR-0.04}{l_1-0.04}\right) 0.01 & N_{1,60,cs} \leq 15 \; AND \; 0.04 \leq CSR \leq l_1 \\ 0.01 + \left(\frac{CSR - l_1}{l_2 - l_1}\right) 0.02 & N_{1,60,cs} \leq 17.5 \; AND \; l_1 \leq CSR \leq l_2 \\ 1.859 \left(1.1 - \sqrt{\frac{N_{1,60,cs}+\Delta n}{46}}\right)^3 \geq 0 & N_{1,60,cs} > 17.5 \; OR \; CSR > l_2 \end{cases}$$

where

$$l_1 = 0.04 + .00207 \, N_{1,60,cs}$$

$$l_2 = 0.04 + .0047 \, N_{1,60,cs}$$

$$\Delta n = N_{1,60,cs} \left(\frac{1}{\left(\frac{CSR - 0.04}{0.56}\right)^{1/3}} - 1 \right)$$

CSR = magnitude corrected cyclic stress ratio. The magnitude correction by Idriss and Boulanger (2008) is recommended.

$$MSF = 6.9 \exp\left(\frac{-M}{4}\right) - 0.058 \leq 1.8$$

Appendix B: Fines Content Correction ΔN_{FC} For Estimation of Strain Potential Index γ_{max}

Faris (2006) recommends an adjustment (increase) to $N_{1,60}$ to account for the effect of non-plastic fines on strain potential. $N_{1,60}$ refers to a standard penetration test (SPT) blow count that is corrected for both overburden stress (normalized to 1 atm) and 60% of theoretical hammer energy. The subscript *cs* is added to signify clean sand conditions. If a soil layer contains silty (non-plastic) fines, $N_{1,60}$ can be adjusted to an equivalent clean sand by adding ΔN_{FC} as shown in equation (B1). ΔN_{FC} is shown in Figure 3.12 and is described numerically in equation (B2) per Faris (2004).

$$N_{1,60,cs} = N_{1,60} + \Delta N_{FC} \tag{B1}$$

$$\Delta N_{FC} \begin{cases} 0.083\, FC - 0.074\, N_{1,60,cs} - 0.417 & if \quad \left(0.882\, N_{1,60,cs} + 5\right) < FC \leq 35 \\ 2.917 - 0.074\, N_{1,60,cs} - 0.417 & if \quad FC > 35 \\ 0 & if \quad FC \leq 0.882\, N_{1,60,cs} + 5 \end{cases} \tag{B2}$$

Appendix C Idriss and Boulanger (2008) Clean Sand Fines Correction

$$(N_1)_{60\,cs} = (N_1)_{60} + \Delta(N_1)_{60} \tag{c1}$$

$$\Delta(N_1)_{60} = Exp[1.63 + \frac{9.7}{FC + 0.01} - \left(\frac{15.7}{FC + 0.01}\right)^2] \tag{c2}$$

In equation (c2), FC is the percent fines smaller than the #200 sieve. This relation is plotted in Figure C1.

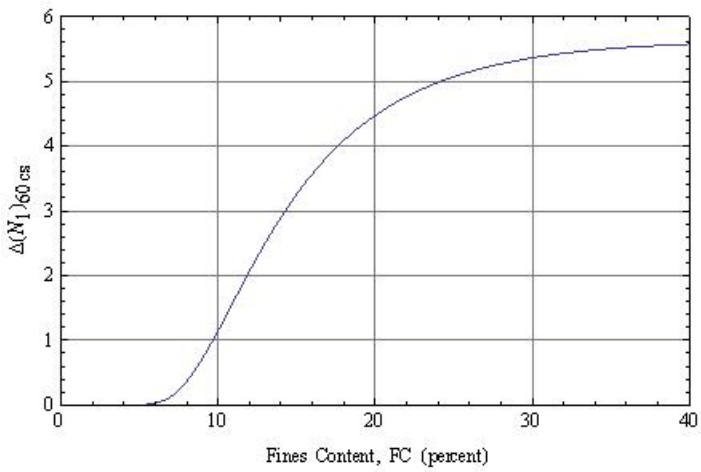

Figure C1. Variation of Δ $(N_1)_{60}$ with fines content (FC) (from Idriss and Boulanger, 2008)